INTERNATIONAL JOURNAL FOR NUMERICAL METHODS IN FLUIDS
Int. J. Numer. Meth. Fluids 2008; **56**:769–803
Published online 7 August 2007 in Wiley InterScience (www.interscience.wiley.com). DOI: 10.1002/fld.1547

On the properties of discrete adjoints of numerical methods for the advection equation

Zheng Liu and Adrian Sandu*, †

Department of Computer Science, Virginia Polytechnic Institute and State University, Blackburg, VA 24060, U.S.A.

SUMMARY

This paper discusses several aspects related to the consistency of the discrete adjoints of upwind numerical schemes. Both linear (finite differences, finite volumes) and nonlinear (slope and flux-limited) discretizations of the one-dimensional advection equation are considered. The analysis is focused on uniform meshes and on explicit numerical schemes. We show that the discrete adjoints may lose consistency near the points where upwinding changes, near inflow boundaries where another numerical scheme is employed, and near the locations where the slope/flux limiter is active in the forward simulation. Numerical results are presented to support the theoretical analysis. Copyright © 2007 John Wiley & Sons, Ltd.

Received 24 July 2006; Revised 9 May 2007; Accepted 14 May 2007

KEY WORDS: discrete adjoint; continuous adjoint; upwinding; slope and flux limiting; consistency

1. INTRODUCTION

Calculation of sensitivities is central to solving many problems in science and engineering, including data assimilation, stability analysis, investigations of various physical mechanisms, optimal control, etc. Our main interest is data assimilation, the process to optimally integrate observational data into models. In a variational approach the data assimilation problem is posed as a minimization problem, which requires the sensitivity (derivatives) of a cost functional with respect to problem parameters [1]. Data assimilation is an essential tool in numerical weather prediction in order to provide accurate forecasts [2].

Adjoint models [3] can efficiently provide gradients of objective functionals that are formulated in terms of the state of a model, and are widely used in conjunction with the optimization of

*Correspondence to: Adrian Sandu, Department of Computer Science, Virginia Polytechnic Institute and State University, Blackburg, VA 24060, U.S.A.
†E-mail: sandu@cs.vt.edu

Contract/grant sponsor: National Science Foundation; contract grant/numbers: ACI-0413872, ITR AP&IM-0205198

large-scale models. There are two ways to derive adjoint models [4]. The continuous ('linearize-then-discretize') approach solves numerically the adjoint equation derived from the forward model. The discrete ('discretize-then-linearize') approach formulates directly the adjoint of the forward numerical scheme. The latter approach is highly attractive since the discrete adjoints, in principle, can be generated completely automatically by reverse-mode automatic differentiation [5].

In this paper we study the consistency of discrete adjoints for numerical schemes used in the solution of hyperbolic conservation laws. These schemes have particular properties such as upwinding, nonlinear stability, etc., and the goal of this research is to understand some of the special issues that appear in the construction of the corresponding discrete adjoints. This topic has important applications in the simulation of the atmosphere and oceans, and in optimal control of fluid flows in engineering applications.

The focus is on conservation laws of the form:

$$\begin{gathered}\frac{\partial c}{\partial t}+\nabla\cdot(f(c))=0, \quad x\in\Omega,\ t^0\leqslant t\leqslant t^{\mathrm{F}} \\ c(t^0,x)=c^0(x), \quad c(t,x)=c^{\mathrm{in}}(t,x)\ \text{ for } x\in\partial\Omega^{\mathrm{in}}\end{gathered} \tag{1}$$

where $c(t,x)$ is the solution ('concentration') field, $\Omega\in\Re^d$ the spatial domain, and $\partial\Omega^{\mathrm{in}}$ the inflow part of the domain boundary. The divergence operator (applied component-wise for systems) is ∇. We consider Dirichlet boundary conditions but the analysis can be easily extended to more general formulations. Equations of the form (1) require special numerical discretization techniques [6–8].

Consider a cost functional that is defined in terms of the solution

$$\mathscr{J}=\int_{t^0}^{t^{\mathrm{F}}}\int_{\Omega} g(c(t,x))\,\mathrm{d}x\,\mathrm{d}t+\int_{\Omega} p(c(t^{\mathrm{F}},x))\,\mathrm{d}x \tag{2}$$

The adjoint equation is a computationally feasible approach to compute the derivatives of the cost functional with respect to initial conditions, boundary values, and model parameters. The adjoint (costate) variables $\lambda(t,x)$ are the solution of the following adjoint problem:

$$\begin{gathered}\frac{\partial\lambda}{\partial t}+\left(\frac{\partial f}{\partial c}\right)^{\mathrm{T}}\cdot\nabla\lambda=-\frac{\partial g}{\partial c}(t,x), \quad x\in\Omega,\ t^{\mathrm{F}}\geqslant t\geqslant t^0 \\ \lambda(t^{\mathrm{F}},x)=\frac{\partial p}{\partial c}(t^{\mathrm{F}},x), \quad \lambda(t,x)=0\ \text{ for } x\in\partial\Omega^{\mathrm{out}}=\partial\Omega-\partial\Omega^{\mathrm{in}}\end{gathered} \tag{3}$$

Here $\partial f/\partial c$ is the Jacobian of the flux function. The homogeneous adjoint boundary condition is due to the fact the cost functional contains no boundary terms. The adjoint problem (3) is solved backwards in time from t^{F} to t^0 to obtain the gradient of the cost functional (2) with respect to the initial conditions

$$\lambda(t^0,x)=\frac{\partial\mathscr{J}}{\partial c^0(x)}$$

Note that the adjoint equation (3) is a linear non-conservative advection equation in the adjoint variable λ. If the forward solution contains discontinuities then (3) is a transport equation with discontinuous coefficients for which meaningful solutions can be defined [9]. The flow speed is given by the eigenvalues of the transposed Jacobian of the flux function, and therefore the

DOI: 10.1002/fld

waves in the adjoint solution travel at the same speed as the waves in the forward solution (but backwards in time). This also implies that the inflow boundary in the adjoint equation is the outflow boundary in the forward equation $\partial\Omega^{\text{out}}$, and explains the formulation of adjoint boundary conditions in (3).

Two approaches are possible to obtain a computational process for the computation of adjoints. In the *continuous adjoint approach* one starts with the exact forward problem (1), formulates the adjoint partial differential equation (3), and solves (3) numerically with the algorithms of choice.

In the *discrete adjoint approach* one starts with a discretization of the forward problem (1), for example,

$$\begin{aligned} &C^{n+1} = C^n + \Delta t\, A(C^n) + B(t^n), \quad C^n, C^{n+1} \in \Re^N, \quad 0 \leqslant n \leqslant M-1 \\ &t^M = t^{\text{F}}, \quad C^0 = C(t^0) \end{aligned} \tag{4}$$

Here A is a discrete version of the flux divergence and B is a boundary condition vector. A numerical cost function that approximates (2) is formulated based on the numerical solution:

$$\mathscr{J}^{\text{d}} = \sum_{n=0}^{M} g(C^n) \tag{5}$$

The discrete adjoint equation corresponding to (4) is

$$\begin{aligned} &\lambda^n = \lambda^{n+1} + \Delta t \left(\frac{\partial A(C)}{\partial C}(t^n) \right)^{\text{T}} \lambda^{n+1} + \frac{\partial g}{\partial C}(C^n) \\ &\lambda \in \Re^N, \quad M-1 \geqslant n \geqslant t^0, \quad \lambda^M = \frac{\partial g}{\partial C}(C^M) \end{aligned} \tag{6}$$

The discrete adjoint variables λ^i in (6) represent sensitivities of the cost functional defined with respect to changes in the ith equation in (4). In particular λ^0 represents those sensitivities with respect to changes in the initial conditions.

It is well accepted that the two approaches lead to different results. Equation (6) can be regarded as a numerical method applied to (3). This 'numerical method' is completely determined by the discretization used for the forward problem, and is not necessarily a consistent and stable scheme for solving the continuous adjoint equation.

Discrete adjoints of upwind numerical methods pose particular challenges. Issues with discrete adjoints can come not only from the hyperbolic discretization, but also from the inclusion in the models of physical processes with parameterized discontinuities [10]. Despite the importance of such schemes in many fields, the impact of discretization techniques for advection/hyperbolic term(s) in the framework of inverse problems and data assimilation has not been extensively studied to date [11].

The construction of adjoints for hyperbolic partial differential equations (PDEs) has been studied theoretically by Giles [12] and Giles *et al*. [13], and Ulbrich [9, 14] and Sei and Symes [15] and Sirkes and Tziperman [4] pointed out that the consistency of the numerical scheme is not automatically inherited by its discrete adjoint. The properties of discrete adjoints for different classes of numerical schemes have been discussed in the literature. They include non-oscillatory advection schemes [16], Euler equations [17], discontinuous Galerkin methods [18], streamline upwind/Petrov Galerkin methods [19], high-resolution methods [11], domain decomposition methods [20], and various advection methods in MITGCM [21]. The correct behaviour of discrete

DOI: 10.1002/fld

adjoints is very important in optimal control of systems with distributed parameters [22, 23] and in data assimilation [24, 25].

The analysis in this paper is limited to the linear advection equation in one dimension

$$\begin{aligned} &\frac{\partial c}{\partial t}+\frac{\partial (uc)}{\partial x}=0, \quad t^0\leqslant t\leqslant t^{\mathrm{F}} \\ &c(t^0,x)=c^0(x) \quad \text{for } x\in\Omega \\ &c(t,x)=c^{\mathrm{in}}(t,x) \quad \text{for } x\in\partial\Omega^{\mathrm{in}} \end{aligned} \tag{7}$$

with a cost function

$$\mathscr{J}=\int_{\Omega} g(c(t^{\mathrm{F}}),x) \tag{8}$$

and the corresponding adjoint equation

$$\begin{aligned} &\frac{\partial \lambda}{\partial t}+u\frac{\partial \lambda}{\partial x}=0, \quad t^{\mathrm{F}}\geqslant t\geqslant t^0 \\ &\lambda(t^{\mathrm{F}},x)=\frac{\partial g}{\partial c}(c(t^{\mathrm{F}}),x) \quad \text{for } x\in\Omega \\ &\lambda(t,x)=0 \quad \text{for } x\in\partial\Omega^{\mathrm{out}} \end{aligned} \tag{9}$$

The forcing term on the right-hand side is zero, but the adjoint has a non-trivial initial value at t^{F}. The cost functional includes no boundary terms. Moreover, no changes in the forward boundaries are allowed which leads to homogeneous adjoint boundary conditions. Here (and throughout the paper) the inflow and the outflow boundaries are defined with respect to the forward model (7).

Advection is the prototype for hyperbolic problems and is in itself a fundamental model with many applications. The results of this paper are relevant for nonlinear problems as well, as many of the features of numerical methods for nonlinear problems are included in the current analysis. The discussion considers the case where the wind field has sources and sinks. These sinks/sources arise in the directional split solutions of multidimensional advection equation and are also important for being able to extend the results to nonlinear systems. The paper also discusses slope/flux-limited nonlinear forward schemes which are widely used to solve nonlinear hyperbolic problems.

The paper is organized as follows. The properties of discrete adjoints for linear finite difference and finite volume discretizations are discussed in Section 2, and for nonlinear slope and flux-limited discretization schemes in Section 3. Numerical examples that support the theoretical findings are presented in Section 4. Conclusions and future research directions are given in Section 5.

2. LINEAR DISCRETIZATION SCHEMES

In this section we study the effects of upwinding and of numerical boundary conditions in the forward scheme on the behaviour of the discrete adjoints. We consider several linear upwind discretizations of (7) and study the consistency of the corresponding discrete adjoint schemes with the continuous equation (9). By 'linear discretization' we mean that the spatial difference operator does not dependend on the solution variables.

DOI: 10.1002/fld

We now analyse the consistency of the discrete adjoints of first and higher order finite difference and finite volume spatial discretizations. The first order method has a short stencil and does not require any change near the boundaries; the high order schemes have longer stencil and require special treatment of the boundaries.

The numerical schemes discussed here are representative for upwind finite differences and volume discretizations. We expect that the discrete adjoints for other schemes, and for other numerical boundary conditions (e.g. non-reflective) will display a similar behaviour as the methods discussed here.

In the subsequent analysis we consider the situation where the cost functional is defined at the final time.

2.1. First order finite differences

Consider the first order upwind scheme:

$$\frac{\partial C_i}{\partial t} = \begin{cases} \dfrac{1}{\Delta x}(U_{i-1}C_{i-1} - U_i C_i) & \text{if } U_i \geqslant 0 \\ \dfrac{1}{\Delta x}(U_i C_i - U_{i+1}C_{i+1}) & \text{if } U_i < 0 \end{cases} \tag{10}$$

Using the notation

$$\gamma_i = \begin{cases} 1 & \text{if } U_i \geqslant 0 \\ 0 & \text{if } U_i < 0 \end{cases} \tag{11}$$

scheme (10) can be written in compact form as

$$\frac{\partial C_i}{\partial t} = \frac{1}{\Delta x}[\gamma_i f_{i-1} + (1 - 2\gamma_i) f_i - (1 - \gamma_i) f_{i+1}] \tag{12}$$

Here $f_i = U_i C_i$ is the flux at the ith node. The Dirichlet boundary conditions are $C_0 = C_{\mathrm{L}}$ and/or $C_{N+1} = C_{\mathrm{R}}$ (only the inflow boundary condition is used). In the following analysis the boundary values are fixed, and consequently the variations of the solution are $\delta C_0 = \delta C_{\mathrm{R}} = 0$. This will lead to homogeneous boundary conditions in the discrete adjoint equation.

Discrete adjoint scheme: The discrete adjoint of (12) is

$$\left(\frac{\partial \lambda}{\partial t}\right)_i = -\frac{U_i}{\Delta x}[-(1 - \gamma_{i-1})\lambda_{i-1} + (1 - 2\gamma_i)\lambda_i + \gamma_{i+1}\lambda_{i+1}] \tag{13}$$

with the boundary condition: $\lambda_0 = \lambda_{N+1} = 0$ (only the inflow boundary condition is used). The adjoint scheme is an upwind discretization of (9).

Consistency inside the domain: Expanding the right-hand side of (13) in Taylor series about the point i

$$\begin{aligned} &\frac{-(1 - \gamma_{i-1})\lambda_{i-1} + (1 - 2\gamma_i)\lambda_i + \gamma_{i+1}\lambda_{i+1}}{\Delta x} \\ &= \frac{\gamma_{i+1} + \gamma_{i-1} - 2\gamma_i}{\Delta x}\lambda_i + (1 + \gamma_{i+1} - \gamma_{i-1})\left(\frac{\partial \lambda}{\partial x}\right)_i + \mathcal{O}(\Delta x) \end{aligned} \tag{14}$$

DOI: 10.1002/fld

leads to the following consistency conditions:

$$\gamma_{i+1} + \gamma_{i-1} - 2\gamma_i = 0, \quad 1 + \gamma_{i+1} - \gamma_{i-1} = 1 \quad \Rightarrow \quad \gamma_{i-1} = \gamma_{i+1} = \gamma_i$$

A necessary condition for consistency of the discrete adjoint scheme is that the wind direction does not change inside the stencil $(i-1, i, i+1)$. Moreover, if there is a wind direction change inside the stencil (e.g. $U_{i-1}<0$ and $U_i, U_{i+1}\geqslant 0$) then $\gamma_{i+1} + \gamma_{i-1} - 2\gamma_i \neq 0$. A continuous wind field (which passes through zero inside the stencil) has a magnitude $U_{i-1}, U_i, U_{i+1} = \mathcal{O}(\Delta x)$. The first term on the right-hand side of (14), which is an error term inconsistent with the equation, is then of magnitude $\mathcal{O}(1)$. A discontinuous wind field (e.g. which jumps from a positive $\mathcal{O}(1)$ value to a negative $\mathcal{O}(1)$ value inside the stencil) will lead to a stronger inconsistent term. For a wind field that is $U = \mathcal{O}(\Delta x^m)$, $m>1$ small around the sign change the strength of the error term is small.

Consistency near the boundary: The numerical boundary conditions of the forward scheme impose the numerical boundary conditions of the discrete adjoint scheme.

Consider the left $(i=0)$ boundary of the forward scheme (12) and assume it as an outflow forward boundary. Under Dirichlet boundary conditions in the forward scheme, the left boundary condition for the discrete adjoint is

$$\frac{\partial \lambda_1}{\partial t} = \frac{U_1}{\Delta x}[(1-2\gamma_1)\lambda_1 + \gamma_2\lambda_2] \tag{15}$$

Since the Dirichlet boundary condition for the discrete adjoint is $\lambda_0 = 0$, the above scheme is formally equivalent to

$$\frac{\partial \lambda_1}{\partial t} = \frac{U_1}{\Delta x}[-(1-\gamma_0)\lambda_0 + (1-2\gamma_1)\lambda_1 + \gamma_2\lambda_2] \tag{16}$$

The discrete adjoint Dirichlet boundary conditions are consistent with the adjoint equation for both the inflow and the outflow situations, provided there is no change of wind direction near the boundary. A similar discussion holds for the right boundary.

In conclusion the discrete adjoint of the first order upwind scheme is inconsistent near sources and sinks, and is consistent near the boundaries. The upwind property of the forward method is preserved by the discrete adjoint scheme.

An alternative interpretation: Consider now the continuous adjoint approach. Specifically we apply the first order upwind scheme (10) to the continuous adjoint PDE (9) to obtain

$$\left(\frac{\partial \mu}{\partial t}\right)_i = -\frac{U_i}{\Delta x}[-(1-\gamma_i)\mu_{i-1} + (1-2\gamma_i)\mu_i + \gamma_i\mu_{i+1}] \tag{17}$$

with the boundary condition: $\mu_0 = \mu_{N+1} = 0$ (only the inflow boundary condition is used).

We now compare the continuous adjoint numerical solution μ with the discrete adjoint solution λ. The discrete adjoint equation (13) can be written as

$$\begin{aligned}\left(\frac{\partial \lambda}{\partial t}\right)_i = &-\frac{U_i}{\Delta x}[-(1-\gamma_i)\lambda_{i-1} + (1-2\gamma_i)\lambda_i + \gamma_i\lambda_{i+1}] \\ &-\frac{U_i}{\Delta x}[(\gamma_{i-1}-\gamma_i)\lambda_{i-1} + (\gamma_{i+1}-\gamma_i)\lambda_{i+1}]\end{aligned} \tag{18}$$

DOI: 10.1002/fld

with the boundary condition: $\lambda_0 = \lambda_{N+1} = 0$ (only the inflow boundary condition is used). The discrete adjoint scheme (18) is the continuous adjoint discretization (17) plus a spurious source term, which becomes non-zero when the wind changes direction ($\gamma_{i-1} \neq \gamma_i$ or $\gamma_i \neq \gamma_{i+1}$).

Consider now the difference between the two adjoints, $\theta_i = \lambda_i - \mu_i$. This difference obeys the equation

$$\left(\frac{\partial \theta}{\partial t}\right)_i = -\frac{U_i}{\Delta x}[-(1-\gamma_{i-1})\theta_{i-1} + (1-2\gamma_i)\theta_i + \gamma_{i+1}\theta_{i+1}] - \frac{U_i}{\Delta x}[(\gamma_{i-1}-\gamma_i)\mu_{i-1} + (\gamma_{i+1}-\gamma_i)\mu_{i+1}] \tag{19}$$

with the final time condition $\theta_i(T) = 0$ and the boundary condition $\theta_0 = \theta_{N+1} = 0$ (only the inflow boundary condition is used).

Assume the continuous adjoint numerical solution (17) converges to the continuous adjoint PDE solution (9) in a certain norm (typically L^2). If $P\lambda_{\text{pde}}$ denotes the restriction of the adjoint PDE solution on the grid (e.g. by taking the solution averages in each cell) we have that

$$\|\mu - P\lambda_{\text{pde}}\| \to 0 \quad \text{when } \Delta x,\ \Delta t \to 0$$

The discrete adjoint solution (18) converges to the continuous adjoint PDE solution if and only if the difference between adjoints converges to zero

$$\|\lambda - P\lambda_{\text{pde}}\| \to 0 \ \Leftrightarrow\ \|\theta\| \to 0 \quad \text{when } \Delta x,\ \Delta t \to 0$$

In practice the wind changes sign at a finite number of points at most. To fix the ideas consider a single wind direction change between gridpoints $i-1$ and i, $\gamma_{i-1} \neq \gamma_i$. Under the assumptions that $U_{i-1}, U_i = \mathcal{O}(\Delta x)$ near the sign change and $\mu_{i-2}, \mu_{i-1} = \mathcal{O}(1)$ the source strength in (19) is $\mathcal{O}(1)$ at the grid points $i-1$ and i, and is zero for all other grid points. In this case the discrete adjoint does not converge in the max norm, but converges in the p-norm ($\|\theta\|_{L^p} \to 0$ for $\Delta x,\ \Delta t \to 0$). If the wind is discontinuous, $U_{i-1}, U_i = \mathcal{O}(1)$ near the sign change, the p-norm convergence may be lost. This indicates that the quality of the discrete adjoint solution may benefit from smoothing the discontinuities (e.g. shocks in the nonlinear case) over several grid cells.

2.2. *Third order finite differences*

We next consider the third order upwind finite difference scheme [26]

$$\frac{\partial C_i}{\partial t} = \begin{cases} \dfrac{1}{\Delta x}\left[-\dfrac{1}{6}f_{i-2} + f_{i-1} - \dfrac{1}{2}f_i - \dfrac{1}{3}f_{i+1}\right] & \text{if } U_i \geqslant 0 \\ \dfrac{1}{\Delta x}\left[\dfrac{1}{3}f_{i-1} + \dfrac{1}{2}f_i - f_{i+1} + \dfrac{1}{6}f_{i+2}\right] & \text{if } U_i < 0 \end{cases} \tag{20}$$

where $f_j = U_j C_j$ is the flux function. The scheme is represented in compact form as

$$\frac{\partial C_i}{\partial t} = \frac{1}{\Delta x}\left[-\frac{\gamma_i}{6}f_{i-2} + \frac{1+2\gamma_i}{3}f_{i-1} + \frac{1-2\gamma_i}{2}f_i + \frac{2\gamma_i - 3}{3}f_{i+1} + \frac{1-\gamma_i}{6}f_{i+2}\right] \tag{21}$$

DOI: 10.1002/fld

The numerical boundary conditions are based on schemes of lower order and with shorter stencils as follows:

$$\frac{\partial C_1}{\partial t} = \begin{cases} \frac{1}{\Delta x}[f_{\mathrm{L}} - f_1] & \text{if } U_1 \geqslant 0 \\ \frac{1}{\Delta x}\left[\frac{3}{2}f_1 - 2f_2 + \frac{1}{2}f_3\right] & \text{if } U_1 < 0 \end{cases}$$
$$= \frac{1}{\Delta x}\left[\gamma_1 f_{\mathrm{L}} + \frac{3-5\gamma_1}{2}f_1 - 2(1-\gamma_1)f_2 + \frac{1-\gamma_1}{2}f_3\right] \tag{22}$$

$$\frac{\partial C_2}{\partial t} = \begin{cases} \frac{1}{\Delta x}\left[-\frac{1}{6}f_{\mathrm{L}} + f_1 - \frac{1}{2}f_2 - \frac{1}{3}f_3\right] & \text{if } U_2 \geqslant 0 \\ \frac{1}{\Delta x}\left[\frac{1}{3}f_1 + \frac{1}{2}f_2 - f_3 + \frac{1}{6}f_4\right] & \text{if } U_2 < 0 \end{cases}$$
$$= \frac{1}{\Delta x}\left[-\frac{\gamma_2}{6}f_{\mathrm{L}} + \frac{1+2\gamma_2}{3}f_1 + \frac{1-2\gamma_2}{2}f_2 + \frac{2\gamma_2-3}{3}f_3 + \frac{1-\gamma_2}{6}f_4\right] \tag{23}$$

The same numerical approach is applied to the right boundary.

Discrete adjoint scheme: In the interior of the domain the discrete adjoint of (21) reads:

$$\left(\frac{\partial \lambda}{\partial t}\right)_i = -\frac{U_i}{\Delta x}\left[\frac{1-\gamma_{i-2}}{6}\lambda_{i-2} + \frac{2\gamma_{i-1}-3}{3}\lambda_{i-1} + \frac{1-2\gamma_i}{2}\lambda_i + \frac{1+2\gamma_{i+1}}{3}\lambda_{i+1} - \frac{\gamma_{i+2}}{6}\lambda_{i+2}\right]$$

The consistency analysis is presented in detail in Appendix A.1. If the wind does not change direction within the stencil $(i-2, i-1, i, i+1, i+2)$ the discrete adjoint scheme (A1) is third order consistent with the continuous adjoint equation. If the wind changes sign within the stencil (not all γ_j are equal) then (A1) is not consistent with the continuous adjoint equation. In the case when the wind speed is smooth a sign change within the stencil $i-2, \ldots, i+2$ implies that $U_j = \mathcal{O}(\Delta x)$ for $j = i-2, \ldots, i+2$ and the zeroth order error term behaves like a spurious source of magnitude $\mathcal{O}(1)$.

As explained in Appendix A.1 the discrete adjoint scheme at the left boundary reads:

$$\frac{\partial \lambda_1}{\partial t} = -\frac{U_1}{\Delta x}\left[\frac{3-5\gamma_1}{2}\lambda_1 + \frac{1+2\gamma_2}{3}\lambda_2 - \frac{\gamma_3}{6}\lambda_3\right]$$

The analysis in Appendix A.1 reveals that the discrete adjoint equation for λ_1 is formally inconsistent with the continuous adjoint for both inflow and outflow situations even if there is no change in the wind direction near the boundary. However, the effects of the outflow inconsistency will not be felt if there is no source in the adjoint equation near the boundary (the cost functional does not use concentration values from near the boundary). In this case $\lambda_1(t) = 0$ and $\partial\lambda_1/\partial t = 0$, which is the correct solution.

DOI: 10.1002/fld

2.3. Finite volumes

We have also studied the consistency of adjoints based on forward finite volume discretizations [26] of the form

$$\frac{\partial C_i}{\partial t} = \frac{1}{\Delta x}(F_{i-1/2} - F_{i+1/2}) \tag{24}$$

The numerical discretization is based on the construction of appropriate approximations of the fluxes through the cell boundaries $F_{i+1/2} \approx U_{i+1/2} C_{i+1/2}$.

The detailed analysis is presented in Appendix A.2. We consider discretizations on staggered grids, where the solution C_i is represented at the centres of the grid cells, and the wind velocity is available at the cell boundaries $U_{i\pm1/2}$. This staggered representation is the main difference between the linear finite volume and the linear finite difference schemes considered in this paper.

The analysis in Appendix A.2 considers two different approximations of the flux, leading to first order and to second order discretization methods, respectively. The consistency analysis reveals that:

- the discrete adjoint is an upwind discretization of the continuous adjoint equation;
- the discrete adjoint of the first order finite volume scheme is consistent with the adjoint equation except for the points where the wind direction changes sign inside the stencil (near flow sinks or sources);
- the discrete adjoint of the first order finite volume scheme is consistent at the boundaries (if there is no change in wind direction);
- the discrete adjoint of the second order finite volume scheme is consistent except for the case when there is a flow sign change within the stencil; and
- the discrete adjoint of the second order finite volume scheme is not consistent at the first two nodes from the boundary.

3. NONLINEAR DISCRETIZATION SCHEMES

This section focuses on nonlinear high-resolution methods. Specifically, we discuss the effects on discrete adjoints introduced by the slope and flux limiting of the forward solution. We consider the case with constant velocity and periodical boundary conditions to leave out the effects of changes in the upwinding pattern and of the numerical boundary conditions which have been discussed in Section 2.

We discuss only a few numerical schemes that we believe are representative for high-resolution finite volume discretizations. There are many discretization techniques that have proved very useful in geoscience applications and are not discussed here. Among them there are the piecewise parabolic method [27] (whose discrete adjoint performance is discussed in [11]), the Rood advection scheme [7], etc. as well as the discontinuous Galerkin approach [18].

3.1. Slope-limited MUSCL scheme

In van Leer's MUSCL scheme [28] the solution is represented as a piecewise linear function, with the concentration in cell i at time t^n having the mean C_i^n and the slope S_i^n.

DOI: 10.1002/fld

The concentrations are advanced in time as follows:

$$\begin{aligned} C_i^{n+1} &= (1-\sigma)C_i^n + \sigma C_{i-1}^n - \delta(\overline{S}_i^n - \overline{S}_{i-1}^n) \\ S_i^{n+1} &= \alpha\overline{S}_i^n + \beta\overline{S}_{i-1}^n + 12\delta(C_i^n - C_{i-1}^n) \end{aligned} \tag{25}$$

where $\sigma = U\Delta t/\Delta x$ is the Courant number and

$$\begin{aligned} &\delta = \frac{\sigma(1-\sigma)}{2}, \quad \alpha = (1-\sigma)(1-2\sigma-2\sigma^2) \\ &\beta = -\sigma(3-6\sigma+2\sigma^2) \end{aligned} \tag{26}$$

In the MUSCL approach the slopes S_i^n are first limited to $\overline{S}_i^n$. We will consider here the van Leer slope limiter [28], which is defined as

$$\overline{S}_i^n = \begin{cases} \min\{\frac{3}{2}|C_i^n - C_{i-1}^n|, |S_i^n|, \frac{3}{2}|C_{i+1}^n - C_i^n|\}\,\mathrm{sign}(S_i^n) \\ \quad \text{if } \mathrm{sign}(C_i^n - C_{i-1}^n) = \mathrm{sign}(S_i^n) = \mathrm{sign}(C_{i+1}^n - C_i^n) \\ 0 \quad \text{otherwise} \end{cases} \tag{27}$$

This definition implies that the slope variables are independent from the solution variables. In other approaches the slopes are derived from concentrations at different cells. In this paper the term 'slope-limited' only refers to the case with independent slope variables.

The forward scheme in the matrix form is

$$\begin{bmatrix} C^{n+1} \\ S^{n+1} \end{bmatrix} = A \cdot \begin{bmatrix} \overline{C}^n \\ \overline{S}^n \end{bmatrix} = A \cdot \begin{bmatrix} C^n \\ L(C^n, S^n) \end{bmatrix} \tag{28}$$

where A is the linear operator of the MUSCL scheme and $\overline{S} = L(C, S)$ is the nonlinear slope limiting operator.

Discrete adjoint scheme: The corresponding discrete adjoint scheme is

$$\begin{bmatrix} \lambda_C^n \\ \lambda_S^n \end{bmatrix} = \begin{bmatrix} I & 0 \\ \dfrac{\partial L}{\partial C} & \dfrac{\partial L}{\partial S} \end{bmatrix}^{\mathrm{T}} \cdot \begin{bmatrix} \overline{\lambda}_C^n \\ \overline{\lambda}_S^n \end{bmatrix} = \begin{bmatrix} I & \left(\dfrac{\partial L}{\partial C}\right)^{\mathrm{T}} \\ 0 & \left(\dfrac{\partial L}{\partial S}\right)^{\mathrm{T}} \end{bmatrix} \cdot A^{\mathrm{T}} \cdot \begin{bmatrix} \lambda_C^{n+1} \\ \lambda_S^{n+1} \end{bmatrix} \tag{29}$$

and therefore

$$\lambda_C^n = \overline{\lambda}_C^n + \left(\frac{\partial L(C^n, S^n)}{\partial C^n}\right)^{\mathrm{T}} \overline{\lambda}_S^n, \quad \lambda_S^n = \left(\frac{\partial L(C^n, S^n)}{\partial S^n}\right)^{\mathrm{T}} \overline{\lambda}_S^n \tag{30}$$

In the adjoint solution, λ_C is the costate variable associated with C, and λ_S the costate associated with S. The case without slope limiter corresponds to $L(C, S) = S$.

3.1.1. Consistency analysis. It is clear from (28) and (29) that in the forward scheme the solution is first slope-limited and then advanced in time, but in the discrete adjoint scheme these steps are

DOI: 10.1002/fld

reversed. The adjoint solution is first propagated (backward in time) with the operator A^{T}

$$\begin{aligned}(\overline{\lambda}_C)_i^n &= (1-\sigma)(\lambda_C)_i^{n+1} + \sigma(\lambda_C)_{i+1}^{n+1} + 12\delta(\lambda_S)_i^{n+1} - 12\delta(\lambda_S)_{i+1}^{n+1} \\ (\overline{\lambda}_S)_i^n &= -\delta(\lambda_C)_i^{n+1} + \delta(\lambda_C)_{i+1}^{n+1} + \alpha(\lambda_S)_i^{n+1} + \beta(\lambda_S)_{i+1}^{n+1}\end{aligned} \tag{31}$$

and then the solution is corrected by the adjoint of the forward limiter (30). Our analysis on the adjoint scheme for finite differences and finite volumes method revealed that the (backward in) time advancement operator A^{T} does not introduce any inconsistency. Therefore, we focus on the adjoint of the limiter operator (30). To simplify the analysis, we assume that there is a single jump discontinuity in the forward solution, and that the slope limiter is active only in the ith cell. The general case where the slope limiter takes different values in different cells can be treated similarly.

A detailed analysis of consistency for each of the four possible values assumed by the van Leer slope limiter (27) is given in Appendix A.3. Here we give a summary of the results:

- *Case 1*: $\overline{S}_i = S_i^n$. The slope is not changed, therefore, this case covers the unlimited situation as well. In this case the consistency of the adjoint is automatic.
- *Case 2*: $\overline{S}_i = 3/2(C_i^n - C_{i-1}^n)$. As a result of slope limiting in the forward problem the local Courant number in the discrete adjoint is changed from σ to $\sigma + 3\delta/2$ in cell i, and from σ to $\sigma - 3\delta/2$ in cell $i-1$. The adjoint mass balance cell $i-1$ is changed with the same amount as the adjoint mass balance cell i but with a different sign, and we expect a wiggle to form in the adjoint solution in the cells $i-1$ and i. Since $\delta = \sigma(1-\sigma)/2$, and the original Courant number $\sigma \in [0, 1]$, the modified Courant numbers are also positive and smaller than one since $\sigma \pm 3\delta/2 \in [0, 1]$. No additional stability conditions are necessary.
- *Case 3*: $\overline{S}_i = 3/2(C_{i+1}^n - C_i^n)$. The local Courant number in the discrete adjoint is changed from σ to $\sigma - 3\delta/2$ in cell i, and from σ to $\sigma + 3\delta/2$ in cell $i+1$. The modified Courant numbers are also positive and smaller than one, $\sigma \pm 3\delta/2 \in [0, 1]$.
- *Case 4*: $\overline{S}_i = 0$. In this case the adjoint of the concentration is not changed, the discrete adjoint is a consistent low order discretization.

3.1.2. Stability analysis. We discuss the method-of-lines stability (MOL-stability). Equation (28) reveals that the forward slope-limited MUSCL scheme is MOL-stable if the Jacobian

$$A \cdot \begin{bmatrix} I & 0 \\ \dfrac{\partial L}{\partial C} & \dfrac{\partial L}{\partial S} \end{bmatrix}$$

has all its eigenvalues of magnitude smaller than or equal one, and the eigenvalues of magnitude one are simple. It is sufficient for MOL-stability of the discrete adjoint (29)–(30) to have A (A^{T}) a stable matrix, since the Jacobian of the slope limiter does not result in increased eigenvalues.

3.2. Flux-limited schemes

Sweby [29] proposed a high-resolution method that averages the first order upwind method and the Lax-Wendroff method. The method for a scalar conservation law is

$$C_i^{n+1} = C_i^n - \frac{\Delta t}{\Delta x}(F_{i+1/2}^n - F_{i-1/2}^n) \tag{32}$$

DOI: 10.1002/fld

where $F_{i\pm1/2}$ are the fluxes through the left/right boundaries of cell i. The numerical flux functions are given by a combination of a low order flux F^{L} and a high order flux F^{H}, defined using a 'flux limiter' function ϕ as follows:

$$F_{i+1/2} = F^{\mathrm{L}}_{i+1/2} + \phi(r_{i+1/2})(F^{\mathrm{H}}_{i+1/2} - F^{\mathrm{L}}_{i+1/2}) \tag{33}$$

In this section we restrict the discussion to the linear advection equation with a constant wind field u. The flux function is $f(C) = uC$. The low order flux F^{L} is given by the first order upwind formula

$$F^{\mathrm{L}}_{i+1/2} = \begin{cases} uC_i & \text{if } u \geqslant 0 \\ uC_{i+1} & \text{if } u < 0 \end{cases} \tag{34}$$

and the high order flux F^{H} is given by the Lax-Wendroff formula

$$F^{\mathrm{H}}_{i+1/2} = \frac{u}{2}(C_{i+1} + C_i - \sigma(C_{i+1} - C_i)) \tag{35}$$

Here $\sigma = u\Delta t/\Delta x$ denotes the Courant number. The flux function (33) becomes

$$F_{i+1/2} = \begin{cases} uC_i + \dfrac{u(1-\sigma)}{2}\phi(r_{i+1/2})(C_{i+1} - C_i) & \text{if } u \geqslant 0 \\ uC_{i+1} - \dfrac{u(1+\sigma)}{2}\phi(r_{i+1/2})(C_{i+1} - C_i) & \text{if } u < 0 \end{cases} \tag{36}$$

The flux limiter function ϕ assumes small values near sharp gradients or local extrema in the solution, therefore, adding numerical diffusion. The limiter value at the interface $i + 1/2$ depends on the ratio $r_{i+1/2}$ of the solution slope upstream of $i + 1/2$ over the solution slope across $i + 1/2$:

$$r_{i+1/2} = \begin{cases} \dfrac{C_i - C_{i-1}}{C_{i+1} - C_i} & \text{if } u \geqslant 0 \\ \dfrac{C_{i+2} - C_{i+1}}{C_{i+1} - C_i} & \text{if } u < 0 \end{cases} \tag{37}$$

We consider four types of flux limiters that are widely used and introduce different amounts of numerical diffusion:

$$\text{Minmod:} \quad \phi(r) = \begin{cases} 0 & \text{if } r < 0 \\ br & \text{if } 0 \leqslant r < 1/b \quad \text{where } 1 \leqslant b \leqslant 2 \\ 1 & \text{if } r \geqslant 1/b \end{cases} \tag{38}$$

$$\text{Superbee:} \quad \phi(r) = \begin{cases} 0 & \text{if } r < 0 \\ 2r & \text{if } 0 \leqslant r < 1/2 \\ 1 & \text{if } 1/2 \leqslant r < 1 \\ r & \text{if } 1 \leqslant r < 2 \\ 2 & \text{if } r \geqslant 2 \end{cases} \tag{39}$$

DOI: 10.1002/fld

$$\text{Van Leer:} \quad \phi(r) = \begin{cases} 0 & \text{if } r<0 \\ 2r/1+r) & \text{if } r \geqslant 0 \end{cases} \tag{40}$$

$$\text{MC:} \quad \phi(r) = \begin{cases} 0 & \text{if } r<0 \\ 2r & \text{if } 0 \leqslant r<1/3 \\ (1+r)/2 & \text{if } 1/3 \leqslant r<3 \\ 2 & \text{if } r \geqslant 3 \end{cases} \tag{41}$$

Adjoint analysis: The derivation of the discrete adjoint of the scheme (32) is given in Appendix A.4. The discrete adjoint scheme reads:

$$\begin{aligned} \lambda_i^n = {} & \lambda_i^{n+1} + \sigma(\lambda_{i+1}^{n+1} - \lambda_i^{n+1}) \\ & - \frac{\sigma(1-\sigma)}{2}[(\phi - r\phi_r)_{i+1/2}^n(\lambda_{i+1}^{n+1} - \lambda_i^{n+1}) - (\phi - r\phi_r)_{i-1/2}^n(\lambda_i^{n+1} - \lambda_{i-1}^{n+1})] \\ & - \frac{\sigma(1-\sigma)}{2}[(\phi_r)_{i+3/2}^n(\lambda_{i+2}^{n+1} - \lambda_{i+1}^{n+1}) - (\phi_r)_{i+1/2}^n(\lambda_{i+1}^{n+1} - \lambda_i^{n+1})] \end{aligned} \tag{42}$$

For the constant wind field case Equation (42) can be written in a conservative form similar to (32):

$$\begin{aligned} \lambda_i^n &= \lambda_i^{n+1} + \frac{\Delta t}{\Delta x}(\mathscr{F}_{i+1/2}^{n+1} - \mathscr{F}_{i-1/2}^{n+1}) \\ \mathscr{F}_{i+1/2}^{n+1} &= u\lambda_{i+1}^{n+1} - u\frac{1-\sigma}{2}(\phi - r\phi_r)_{i+1/2}^n(\lambda_{i+1}^{n+1} - \lambda_i^{n+1}) \\ &\quad - u\frac{1-\sigma}{2}(\phi_r)_{i+3/2}^n(\lambda_{i+2}^{n+1} - \lambda_{i+1}^{n+1}) \\ &= u\lambda_{i+1}^{n+1} - u\frac{1-\sigma}{2}[(\phi - r\phi_r)_{i+1/2}^n + (\phi_r)_{i+3/2}^n\rho_{i+1/2}^{n+1}](\lambda_{i+1}^{n+1} - \lambda_i^{n+1}) \end{aligned}$$

where ρ is the slope ratio (37) for the adjoint variable

$$\rho_{i+1/2}^{n+1} = \frac{\lambda_{i+2}^{n+1} - \lambda_{i+1}^{n+1}}{\lambda_{i+1}^{n+1} - \lambda_i^{n+1}}$$

The application of Sweby's flux-limited scheme (A16) to the continuous adjoint equation leads to the following numerical continuous adjoint formulation:

$$\begin{aligned} \lambda_i^n &= \lambda_i^{n+1} + \frac{\Delta t}{\Delta x}(\overline{\mathscr{F}}_{i+1/2}^{n+1} - \overline{\mathscr{F}}_{i-1/2}^{n+1}) \\ \overline{\mathscr{F}}_{i+1/2}^{n+1} &= u\lambda_{i+1}^{n+1} - u\frac{1-\sigma}{2}\phi(\rho_{i+1/2}^{n+1})(\lambda_{i+1}^{n+1} - \lambda_i^{n+1}) \end{aligned} \tag{43}$$

where the adjoint limiter values are computed based on differences of the adjoint variable $\phi(\rho)$.

DOI: 10.1002/fld

The discrete adjoint flux equation (43) has the form of the flux-limited discretization of the continuous adjoint equation with the limiter function replaced by

$$\phi(\rho_{i+1/2}^{n+1}) \quad \longrightarrow \quad \varphi(\rho_{i+1/2}^{n+1}) = (\phi - r\phi_r)_{i+1/2}^{n} + (\phi_r)_{i+3/2}^{n}\rho_{i+1/2}^{n+1}$$

Consequently, scheme (42) is consistent with the continuous adjoint equation if the adjoint slope $\rho_{i+1/2}^{n+1}$ is bounded. If the adjoint slope is not bounded in areas where the forward limiter is active (e.g. sensors of the forward solution are placed in areas of sharp gradients) then scheme (42) may lose consistency. For the limiter in the forward calculation kept fixed to a constant value we obtain a constant value of the limiter in the discrete adjoint $\varphi = \phi = \text{const}$. Thus, the discrete adjoint of the first order scheme is the first order scheme, and the discrete adjoint of Lax-Wendroff is the Lax-Wendroff scheme.

An interesting situation occurs when the limiter function is active. For the limiter functions discussed here $\phi_r \geqslant 0$. For $\rho_{i+1/2}^{n+1} < 0$ the discrete adjoint 'limiter' can take negative values $\varphi < 0$, and thus its behaviour does not help the nonlinear stability properties (for which one would require $\varphi = 0$). Moreover, if the forward limiter is in a non-constant regime then $\phi_r \neq 0$ and $\rho \to \infty \Rightarrow \varphi(\rho) \to \infty$. Thus, near sharp gradients the discrete adjoint scheme will add a large multiple of 'antidiffusive' adjoint flux; we therefore expect the discrete adjoint solution to display considerable spurious oscillations.

Smooth adjoint solution: We next assume a smooth adjoint variable λ (in the sense that $\rho \approx 1$) and take the limit of Equation (42) for $\Delta t \to 0$, $\Delta x \to 0$ with $\sigma = \text{const}$. The first term gives a first order upwind discretization, which converges to the continuous adjoint equation since there are no changes in the upwind pattern and no changes in the boundary conditions. The other terms should account for possible discontinuities in the forward limiter.

The limit reveals that the discrete adjoint variables satisfy the following modified equation:

$$\lambda_t + u\lambda_x = \frac{1-\sigma}{2}([\phi - r\phi_r] - [\phi_r]_+)u\lambda_x \tag{44}$$

where $[\xi]$ is the magnitude of the jump of the function ξ at a given location x (the jump is equal to zero for continuous functions). $[\xi]_+$ is the magnitude of the jump at x_+ (infinitesimally to the right of the given location). The modified equation is the continuous adjoint equation with an additional pseudo-source driven by discontinuities of ϕ, ϕ_r, $r\phi_r$. These three functions depend the forward solution. Note that even if the forward solution is smooth a jump in the limiter can occur (e.g. at an extremum of the forward solution, or for values of a slope ratio for which the limiter formula is nondifferentiable).

In smooth regions of the forward solution the limiter assumes a constant value (the maximum), the jumps of the limiter are zero, and the above modified equation is the same as the continuous adjoint equation. In regions where the adjoint solution is constant $\lambda_x = 0$ and the source term vanishes.

Consider now the source term near a discontinuity (or sharp gradient), a local maximum or a local minimum of the forward solution. At these points the forward limiter becomes active, discontinuities may appear in ϕ, ϕ_r, $r\phi_r$, and the source term becomes non-zero. Because the adjoint solution is propagated backwards with the same speed as the forward solution, the effects of the source term will tend to accumulate in the same region of the adjoint (corresponding to the discontinuity of the forward solution). This accumulation can cause growing wiggles in the adjoint

DOI: 10.1002/fld

variable, as well as considerable phase offset. To understand the phase offset we rewrite (44) as

$$\lambda_t + u\left(1 - \frac{1-\sigma}{2}[\phi - r\phi_r] + \frac{1-\sigma}{2}[\phi_r]_+\right)\lambda_x = 0 \tag{45}$$

which shows that the local adjoint solution speed is changed due to action of the forward limiter.

4. NUMERICAL EXAMPLES

We now solve the advection equation for different wind fields, initial concentrations, and final adjoint profiles using the discrete adjoints of the methods analysed in the previous two sections. The spatial domain considered $x \in [0, 2]$ is discretized with a uniform grid with the grid size $\Delta x = 0.02$. The time step is $\Delta t = 0.005$ (all in a dimensional units).

4.1. Discrete adjoints of first order linear spatial discretizations

To test the discrete adjoints of linear advection spatial discretizations we first prescribe a smooth adjoint field at the final time:

$$\lambda(t^{\mathrm{F}}, x) = 0.2 + 0.2\,\sin(2\pi x)$$

We also consider two different wind fields as follows:

1. $U^A(x) = 0.5 - 0.5x$. This wind field has a sink of zero velocity at $x = 1$, and two inflow boundary conditions (at $x = 0$ and 2); and
2. $U^B(x) = -0.5 + 0.5x$. This wind field has a source of zero velocity at $x = 1$, and two outflow boundary conditions (at $x = 0$ and 2).

Note that $|U^A|, |U^B| \leqslant \frac{1}{2}$ and therefore the Courant numbers of the simulation are small, $\sigma \leqslant \frac{1}{8}$.

The results of the adjoint integration for $2 \geqslant t \geqslant 0$ with the discrete adjoint of the first order finite difference scheme are presented in Figures 1 and 2. Both figures reveal spikes in the discrete adjoint solution at $x = 1$ due to the inconsistency of the discrete adjoint near the sink (Figure 1) or source (Figure 2). The method is consistent for both inflow (Figure 1) and outflow (Figure 2) boundaries, and the discrete adjoints have the desired values in a neighbourhood of the boundaries.

4.2. Discrete adjoints of third order linear spatial discretizations

Figures 3 and 4 show the results of the same problem integrated backwards with the discrete adjoint of the third order finite difference scheme. Both figures show spikes in the discrete adjoint solution at $x = 1$, confirming the inconsistency of the scheme near sinks (Figure 3) and sources (Figure 4). The third order discrete adjoint is inconsistent near inflow boundaries and this is shown by the boundary spikes in Figure 3. Since there are no observations near the outflow boundaries in Figure 4 the inconsistency does not affect the solution, which has the correct zero value.

4.3. Discrete adjoints of the slope-limited method

For the slope-limited scheme we consider the advection equation with periodic boundary conditions and a constant wind field $u = 0.8$. This setting eliminates the possible inconsistencies due to

DOI: 10.1002/fld

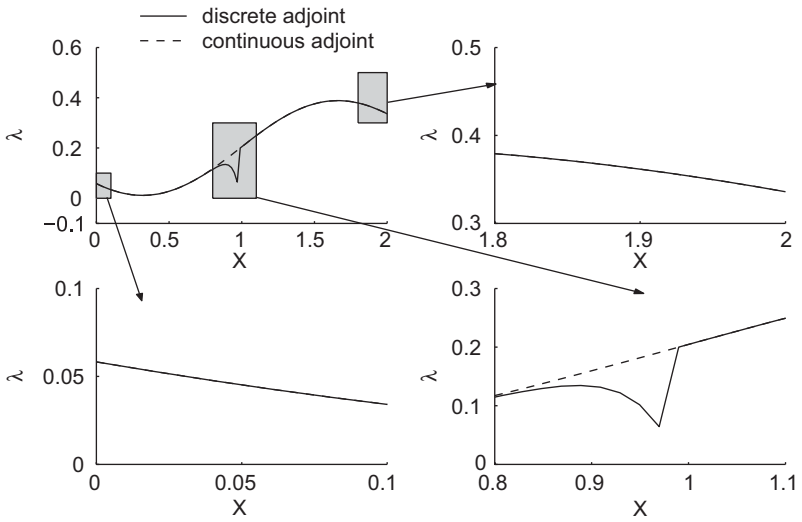

Figure 1. The discrete adjoint solution for first order scheme and wind field $U^A(x) = 0.5 - 0.5x$. The spike is due to the inconsistency near the sink ($x = 1$).

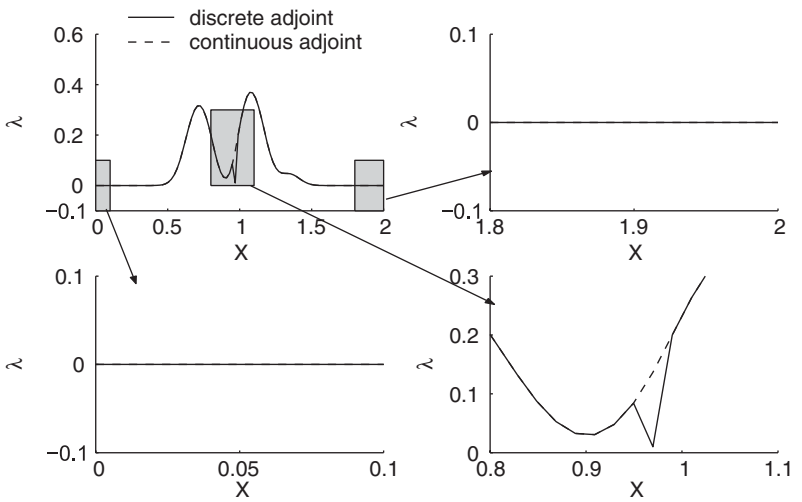

Figure 2. The discrete adjoint solution for first order scheme and wind field $U^B(x) = -0.5 + 0.5x$. The spike is due to the inconsistency near the source ($x = 1$).

boundary conditions and the ones due to changes in upwind pattern, and allows the focus to be on inconsistencies arising from slope limiting. The time interval is $t \in [0, 4]$. The adjoints are integrated backwards and shown at $t = 0.285$.

The behaviour of the limiter at each cell is indicated by the 'limiter state', which has the value $\{0, 0.5, 1.0, 1.5\}$ when the limited slope is calculated as $\overline{S}_i = \{S_i, C_i - C_{i-1}, C_{i+1} - C_i, 0\}$, respectively. A non-zero value means that slope limiting is active at that point.

DOI: 10.1002/fld

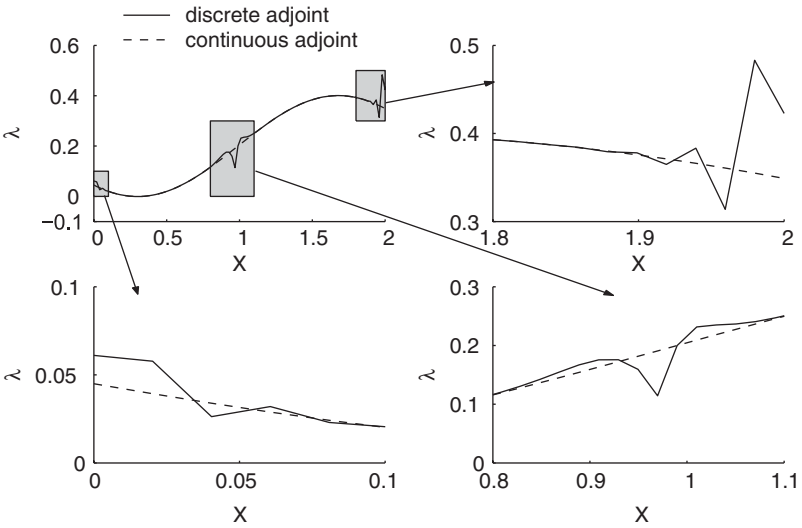

Figure 3. The discrete adjoint solution for third order scheme and wind field $U^A(x) = 0.5 - 0.5x$. The spikes are due to the inconsistency near the sink ($x = 1$) and near inflow boundaries ($x = 0$ and 2).

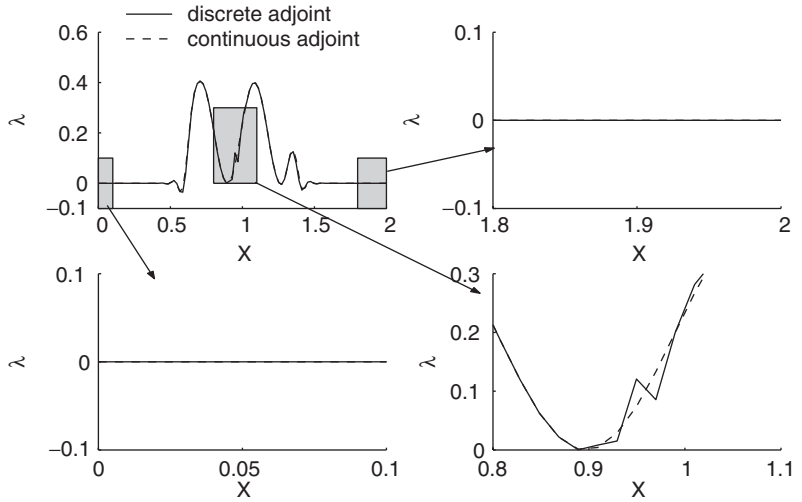

Figure 4. The discrete adjoint solution for third order scheme and wind field $U^B(x) = -0.5 + 0.5x$. The spike is due to the inconsistency near the source ($x = 1$).

First, we consider a square wave forward solution, which forces the slope limiter to be active at its edges. The adjoint is initialized to a non-smooth profile at the final time (equal to the final state of the forward solution). Since the features of the adjoint travel at the same speed as the

DOI: 10.1002/fld

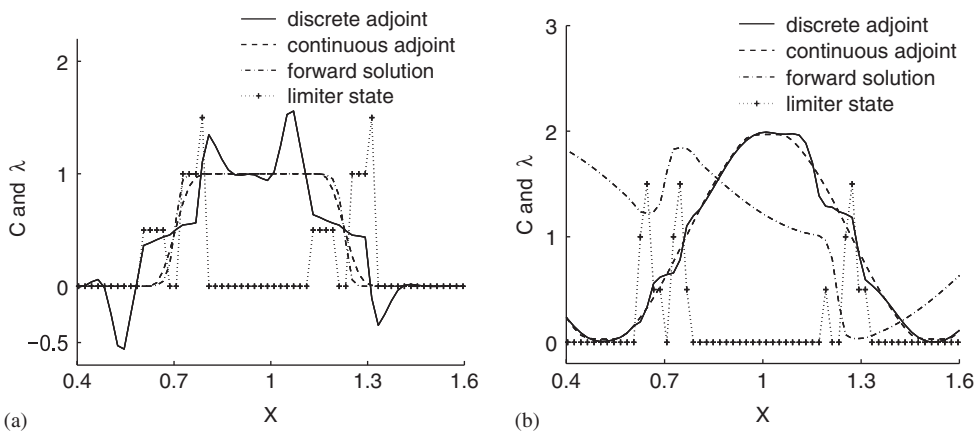

Figure 5. The discrete adjoint of the slope-limited MUSCL scheme is not consistent with the continuous adjoint at grid cells where the limiter is active (limiter type is not 0): (a) square wave forward solution and non-smooth adjoint and (b) sine plus square wave forward solution and smooth adjoint.

features of the forward solution, the sharp gradients of the adjoint and of the forward solution overlap at all times. Figure 5(a) shows the inconsistency of the discrete adjoint solutions near the discontinuities of the forward solution.

For limiter state equal to 0.5 (case 2 in Section 3.1.1) the local Courant number is changed from σ to $\sigma+3\sigma(1-\sigma)/4$ in cell i, and from σ to $\sigma-3\sigma(1-\sigma)/4$ in cell $i-1$. According to (A13) when the limiter is active in cell i the adjoint variable in that cell is changed to $\lambda_i + 3\delta/2(\lambda_{i+1} - \lambda_i)$, and in cell $i-1$ is changed to $\lambda_i - 3\delta/2(\lambda_{i+1} - \lambda_i)$. For the left edge of the wave $\lambda_{i+1} \geqslant \lambda_i$ and the discrete adjoint solution is increased when the limiter is active, and decreased to the left. This wiggle is visible at $x \approx 0.7$. For the right edge of the wave $\lambda_{i+1} \leqslant \lambda_i$ and the solution is decreased when the limiter is active, but is increased to the left. This can be seen on the right edge of the square wave at $x \approx 1.2$.

For limiter state equal to 1 (case 3 in Section 3.1.1) the local Courant number is changed from σ to $\sigma-3\sigma(1-\sigma)/4$ in cell i, and from σ to $\sigma+3\sigma(1-\sigma)/4$ in cell $i+1$. Following Equation (A14) when the limiter is active in cell i the adjoint variable in that cell is changed to $\lambda_i - 3\delta/2(\lambda_{i+1} - \lambda_i)$, and in cell $i+1$ is changed to $\lambda_i + 3\delta/2(\lambda_{i+1} - \lambda_i)$. For the left edge of the wave $\lambda_{i+1} \geqslant \lambda_i$ and the discrete adjoint solution is decreased when the limiter is active, and increased to the right. This wiggle is visible at $x \approx 0.8$. For the right edge of the wave $\lambda_{i+1} \leqslant \lambda_i$ and the solution is increased when the limiter is active, but is decreased to the right. This can be seen on the right edge of the square wave at $x \approx 1.3$.

Next we consider the forward solution as a square wave superimposed over a sine function, which forces the slope limiter to be active at the square wave edges and also at the minima/maxima. The adjoint solution is initialized with a smooth sine function. The results in Figure 5(b) show how the scheme loses consistency when the limiter is active. Confirming the analysis in Section 3.1.1 the amplitude of the wiggles is smaller since the effect of the limiter depends on the increments $(\lambda_{i+1} - \lambda_i)$ in the adjoint.

DOI: 10.1002/fld

4.4. *Discrete adjoints of flux-limited methods*

For the flux-limited scheme we consider the advection equation with periodic boundary conditions and a constant wind field $u = 1$. This setting eliminates the possible inconsistencies due to boundary conditions and the ones due to changes in upwind pattern, and allows the focus to be on inconsistencies arising from flux limiting. The time interval is $t \in [0, 1]$. The adjoint solution is integrated backwards and plotted at $t = 0.5$.

In the first test the initial forward solution is given by the superposition of a square wave and a small sine function

$$C(x, 0) = \begin{cases} 2 + 0.1(1 + \cos(\pi x/2)) & \text{for } x \in [0.2, 0.6] \\ 0.1(1 + \cos(\pi x/2)) & \text{for } x \in [0, 0.2) \cup (0.6, 2] \end{cases}$$

The small sine prevents spurious jumps of the flux limiter due to roundoff error size differences in the (constant) solution at neighbouring cells.

The results are shown in Figure 6. For each scheme the discrete adjoint solution is shown together with the reference continuous adjoint, the forward solution, and the limiter values. For unlimited solutions (using either the low order or the high order flux function, see Figures 6(a) and (b)) the limiter value is constant. The discrete adjoint is consistent with the continuous adjoint equation. For the minmod, superbee, van Leer, and MC flux limiters (Figures 6(c), (d), (e), and (f), respectively) jumps in the limiter value act as spurious sources and lead to the formation of wiggles in the discrete adjoint solution.

An interesting situation arises when the forward solution is constant over a space interval. Small variations in the solution value (of the order of roundoff) lead to order one changes in the solution slope ratio r, which are 'sensed' by the limiter. Jumps in the limiter value lead to spurious sources that accumulate over time and can have a significant effect over the discrete adjoint. As an example, we initialize the forward solution to a square wave

$$C(x, 0) = \begin{cases} 2 & \text{for } x \in [0.2, 0.6] \\ 0 & \text{for } x \in [0, 0.2) \cup (0.6, 2] \end{cases}$$

Note that the forward solution is not much different than in the previous example. However, the discrete adjoints for the superbee and MC limiters show significant wiggles as illustrated in Figure 7. The van Leer and minmod limiters are not affected as much by this phenomenon.

In order to simulate a data assimilation experiment with observations at the final time $t^{\mathrm{F}} = 1$ at locations $x_{\mathrm{obs}} \in \{0.1, 0.3, 0.5, 0.7, 0.9\}$ we initialize the adjoint with 1 at $x = x_{\mathrm{obs}}$ and zero otherwise. These spikes (influence regions) are advected backwards in time. The results are shown in Figure 8. The numerical solution of the continuous adjoint equation consists of wider spikes due to numerical diffusion. The discrete adjoint solution displays spurious wiggles that are larger near the discontinuities of the forward solution. This is the result of excessive antidiffusive fluxes introduced in the adjoint solution where the forward limiter is active. The position

DOI: 10.1002/fld

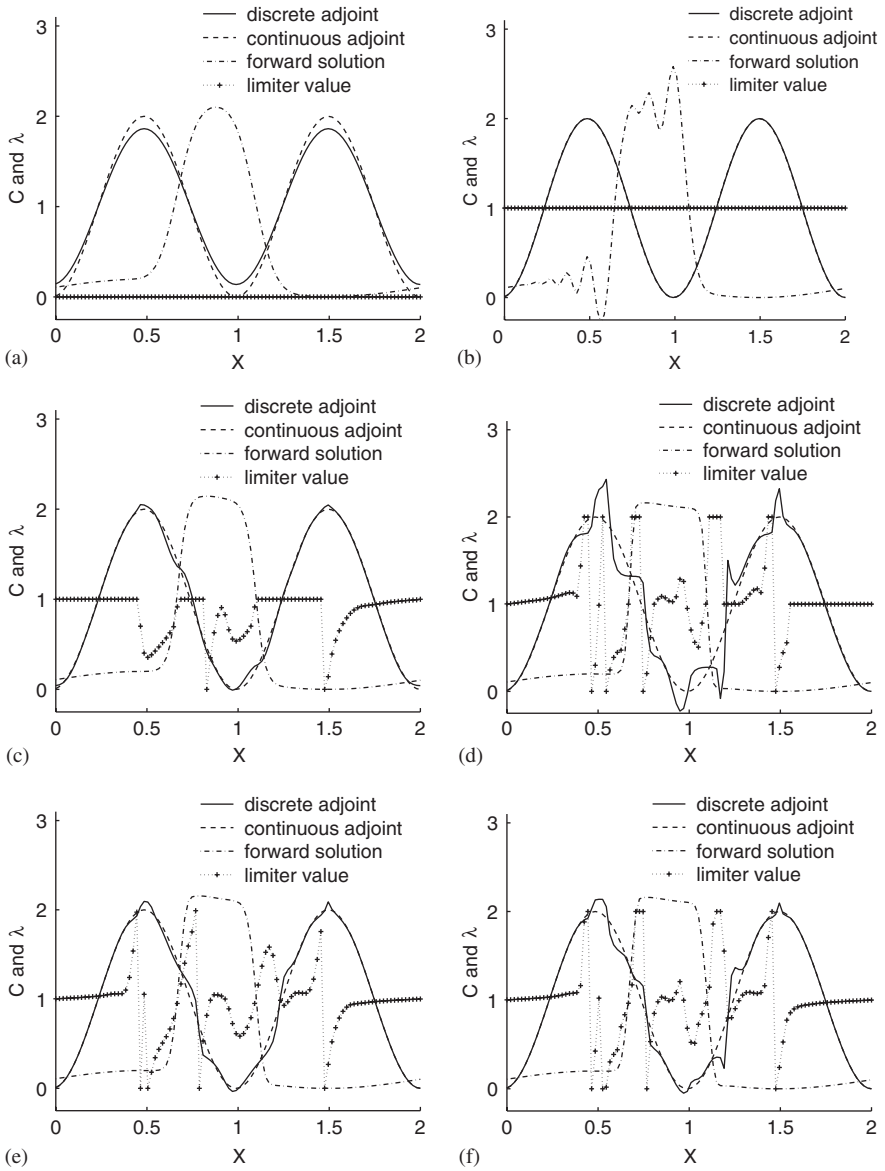

Figure 6. The discrete adjoint solutions at $t = 0.5$ for different flux limiters. Also shown are the continuous adjoint, the forward solution, and the value of the limiter. Jumps in the limiter values lead to the formation of wiggles in the discrete adjoint. The discrete adjoint is not consistent with the continuous adjoint near sharp gradients in the forward solution: (a) first order upwind scheme; (b) Lax-Wendroff scheme; (c) minmod flux limiter; (d) superbee flux limiter; (e) Van Leer flux limiter; and (f) MC flux limiter.

DOI: 10.1002/fld

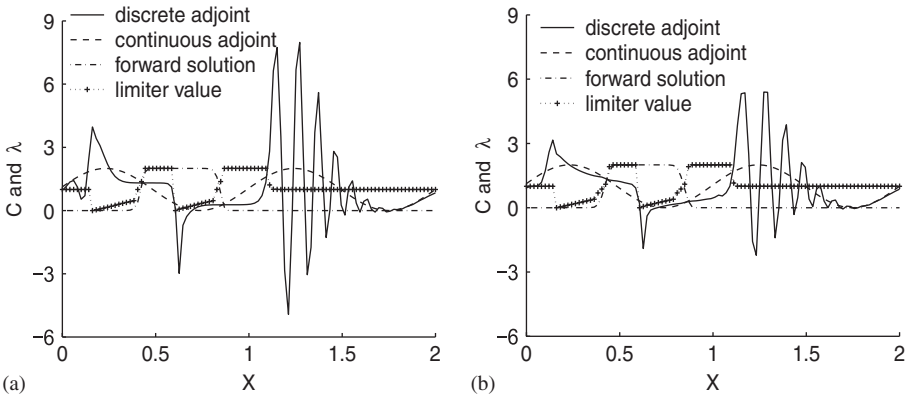

Figure 7. The discrete adjoint solutions at $t = 0.5$ for the superbee and minmod flux limiters. Large constant regions of the forward solution lead to small spurious changes in the limiter value, which act as a spurious source. The cumulative effects of these sources on the discrete adjoint solution can be significant: (a) superbee flux limiter and (b) MC flux limiter.

of the spikes is slightly shifted for the superbee limiter, but is correct for van Leer and MC limiters.

5. CONCLUSIONS

In this paper we discuss several properties of the discrete adjoints of linear and nonlinear advection schemes. We consider first and third order upwind finite differences, first and second order finite volumes, the MUSCL slope-limited scheme, and the flux-limited scheme of Sweby with several limiter functions.

The analysis of finite difference methods reveals that both the changes of direction in the wind field and the numerical boundary scheme lead to changes in the computational pattern of the forward scheme. This results in changes in the pattern of the discrete adjoint that do not preserve consistency. The discrete adjoints are pointwise inconsistent with the continuous adjoint equations at inflow boundaries and near sinks or sources (i.e. points where the wind field changes sign).

Slope limiting in the forward MUSCL scheme results in a change of the local Courant number in the discrete adjoint. Specifically, the local Courant number is increased (decreased) in the cell where the limiter is active, and is decreased (increased) by the same amount in a neighbouring cell. This leads to the formation of a wiggle, with the solution being artificially increased in one cell, and artificially decreased in a neighbouring cell.

The discrete adjoint of a flux-limited forward scheme has the form of another flux-limited scheme applied to the continuous adjoint equation. The discrete adjoint 'limiter' function depends on the forward limiter values, and will add a large multiple of antidiffusive adjoint flux near sharp gradients in the forward solution. This may lead to considerable spurious oscillations in the discrete adjoint solution. For smooth adjoint solutions the action of the forward flux limiter can be represented as an artificial source in the adjoint equation, whose magnitude is proportional to the jump of the limiter function ϕ and its derivatives, the wind velocity, and the derivative of the

DOI: 10.1002/fld

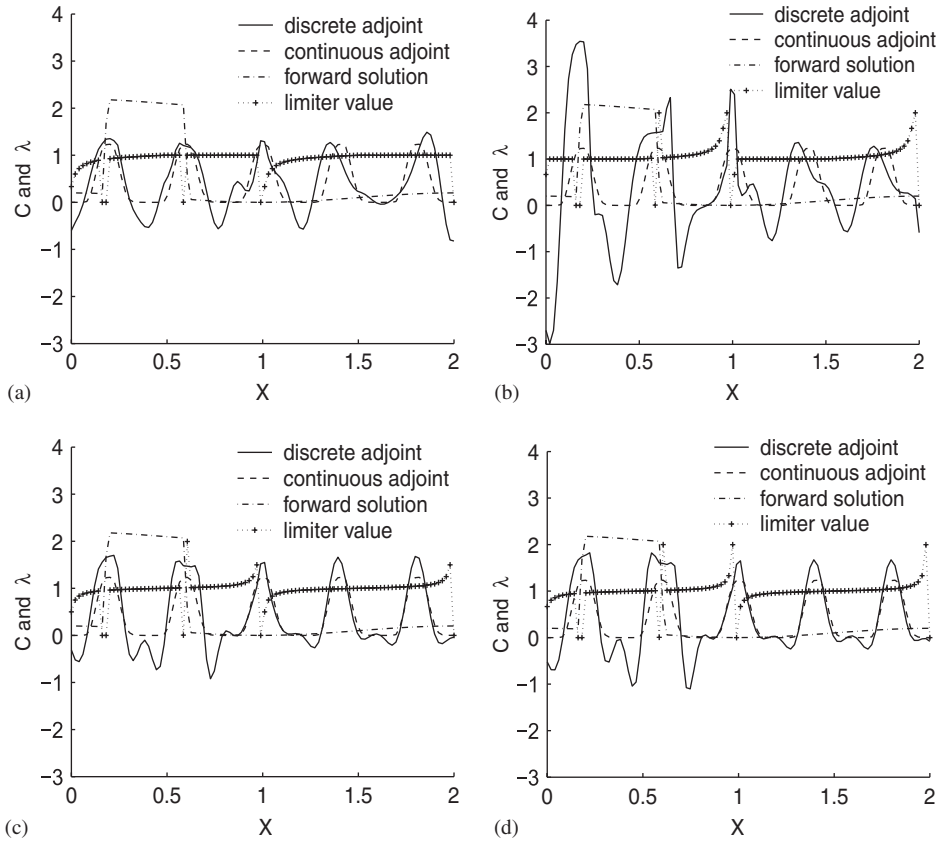

Figure 8. The discrete adjoint solutions at $t = 0.5$ for different flux limiters. The adjoints are initialized to 1 for $x \in \{0.1, 0.3, 0.5, 0.7, 0.9\}$ and zero otherwise: (a) minmod flux limiter; (b) superbee flux limiter; (c) Van Leer flux limiter; and (d) MC flux limiter.

adjoint solution $[\phi - r\phi_r - \phi_r]u\lambda_x$. The effects of this source are larger where there are large changes of the slope of the forward solution r, and where the adjoint solution has sharp spatial gradients. In particular, having observations near the sharp gradients of the forward solution leads to large jumps in the limiter $[\phi]$ and to large adjoint gradients λ_x, and may lead to artificially large values of the sensitivity coefficient.

Future work will extend the analysis to discrete adjoints for nonlinear hyperbolic equations, and for multi-dimensional systems. The extension to multiple dimensions can be done *via* a dimensional splitting (in which case the current conclusions apply directly) or *via* multidimensional schemes (in which case an extension of the current analysis is necessary). We will investigate the possibility to construct upwind and limited forward schemes which lead to consistent discrete adjoints.

We plan to assess how the inconsistency and instability of the discrete adjoints affect the performance of the optimization procedure in the solution of inverse problems, especially data assimilation. The quality of the analysis in regions of sharp gradients may be deteriorated by the

DOI: 10.1002/fld

spurious oscillations if discrete adjoints are used. Moreover, the properties of the high-resolution numerical discretizations may cause some cost functions to be non-smooth (e.g. with respect to the initial conditions). This, together with the spurious oscillations in the discrete adjoint, may require the use of non-smooth optimization techniques (like the one employed in [24]).

APPENDIX A

A.1. Consistency of the third order finite difference discrete adjoint

In this section we analyse the consistency of the discrete adjoint of the third order finite difference scheme (21).

Consistency inside the domain: In the interior of the domain the discrete adjoint of (21) reads:

$$\left(\frac{\partial\lambda}{\partial t}\right)_i = -\frac{U_i}{\Delta x}\left[\frac{1-\gamma_{i-2}}{6}\lambda_{i-2} + \frac{2\gamma_{i-1}-3}{3}\lambda_{i-1} + \frac{1-2\gamma_i}{2}\lambda_i + \frac{1+2\gamma_{i+1}}{3}\lambda_{i+1} - \frac{\gamma_{i+2}}{6}\lambda_{i+2}\right] \tag{A1}$$

To analyse consistency expand (A1) in Taylor series in space about cell i:

$$\begin{aligned}\left(\frac{\partial\lambda}{\partial t}\right)_i = -U_i\Bigg[&-\frac{1}{6\Delta x}(\gamma_{i-2}-4\gamma_{i-1}+6\gamma_i-4\gamma_{i+1}+\gamma_{i+2})\\ &+\frac{1}{3}(\gamma_{i-2}-2\gamma_{i-1}+3+2\gamma_{i+1}-\gamma_{i+2})\left(\frac{\partial\lambda}{\partial x}\right)_i\\ &+\frac{\Delta x}{3}(-\gamma_{i-2}+\gamma_{i-1}+\gamma_{i+1}-\gamma_{i+2})\left(\frac{\partial^2\lambda}{\partial x^2}\right)_i\\ &+\frac{\Delta x^2}{9}(2\gamma_{i-2}-\gamma_{i-1}+\gamma_{i+1}-2\gamma_{i+2})\left(\frac{\partial^3\lambda}{\partial x^3}\right)_i+\mathcal{O}(\Delta x^3)\Bigg]\end{aligned}$$

Since all $\gamma_j \in \{0, 1\}$ the zeroth order consistency condition is satisfied if and only if the wind does not change direction within the stencil $(i-2, i-1, i, i+1, i+2)$,

$$\gamma_{i-2}-4\gamma_{i-1}+6\gamma_i-4\gamma_{i+1}+\gamma_{i+2}=0 \quad\Leftrightarrow\quad \gamma_{i-2}=\gamma_{i-1}=\gamma_i=\gamma_{i+1}=\gamma_{i+2}$$

In this case it can be seen that the $\mathcal{O}(\Delta x^{-1})$, $\mathcal{O}(\Delta x)$, and $\mathcal{O}(\delta x^2)$, terms all vanish and the discrete adjoint scheme (A1) is third order consistent with the continuous adjoint equation.

If the wind changes sign within the stencil (not all γ_j are equal) then (A1) is not consistent with the continuous adjoint equation. In the case when the wind speed is smooth a sign change within the stencil $i-2, \ldots, i+2$ implies that $U_i = \mathcal{O}(\Delta x)$. From the Taylor series we infer that the zeroth order term behaves like a spurious source of magnitude $\mathcal{O}(1)$.

DOI: 10.1002/fld

Consistency near the boundary: We first consider the left boundary. The coefficient matrix for the forward spatial discretization is

$$A=\frac{1}{\Delta x}\begin{bmatrix} \frac{3-5\gamma_1}{2}U_1 & (2\gamma_1-2)U_2 & \frac{1-\gamma_1}{2}U_3 & 0 & 0 & \cdots \\ \frac{1+2\gamma_2}{3}U_1 & \frac{1-2\gamma_2}{2}U_2 & \frac{2\gamma_2-3}{3}U_3 & \frac{1-\gamma_2}{6}U_4 & 0 & \cdots \\ -\frac{\gamma_3}{6}U_1 & \frac{1+2\gamma_3}{3}U_2 & \frac{1-2\gamma_3}{2}U_3 & \frac{2\gamma_3-3}{3}U_4 & \frac{1-\gamma_3}{6}U_5 & \cdots \\ 0 & -\frac{\gamma_4}{6}U_2 & \frac{1+2\gamma_4}{3}U_3 & \frac{1-2\gamma_4}{2}U_4 & \frac{2\gamma_4-3}{3}U_5 & \cdots \\ & & \vdots & & & \end{bmatrix}$$

The adjoint scheme at the left boundary reads:

$$\frac{\partial\lambda_1}{\partial t}=-\frac{U_1}{\Delta x}\left[\frac{3-5\gamma_1}{2}\lambda_1+\frac{1+2\gamma_2}{3}\lambda_2-\frac{\gamma_3}{6}\lambda_3\right]$$

If $U_1\geqslant 0$ ($\gamma_1=1$) the left is an inflow boundary (in the forward problem), and there is no adjoint boundary condition to impose.

$$\frac{\partial\lambda_1}{\partial t}=-\frac{U_1}{\Delta x}\left[-\lambda_1+\frac{1+2\gamma_2}{3}\lambda_2-\frac{\gamma_3}{6}\lambda_3\right]$$

A Taylor series around x_1 leads to:

$$\left(\frac{\partial\lambda}{\partial t}\right)_1=-U_1\left[\frac{11+4\gamma_2-\gamma_3}{6\Delta x}+\frac{-2-4\gamma_2+2\gamma_3}{6}\left(\frac{\partial\lambda}{\partial x}\right)_1+\mathcal{O}(\Delta x)\right]$$

Since $\gamma_2, \gamma_3\in\{0, 1\}$ the discrete adjoint equation for λ_1 is inconsistent with the continuous adjoint.

If $U_1<0$ ($\gamma_1=0$) the left is an outflow boundary (in the forward problem), and the inflow adjoint condition $\lambda_0=0$ needs to be used. The discrete adjoint equation reads

$$\frac{\partial\lambda_1}{\partial t}=-\frac{U_1}{\Delta x}\left[\frac{\alpha}{6}\lambda_0+\frac{3}{2}\lambda_1+\frac{1+2\gamma_2}{3}\lambda_2-\frac{\gamma_3}{6}\lambda_3\right]$$

DOI: 10.1002/fld

where a multiple of the boundary condition $\lambda_0 = 0$ has been added. A Taylor series around x_1 leads to:

$$\left(\frac{\partial\lambda}{\partial t}\right)_1 = -U_1\left[\frac{11+\alpha+4\gamma_2-\gamma_3}{6\Delta x}+\frac{2-\alpha+4\gamma_2-2\gamma_3}{6}\left(\frac{\partial\lambda}{\partial x}\right)_1 + \frac{2+\alpha+4\gamma_2-4\gamma_3}{12}\Delta x\left(\frac{\partial^2\lambda}{\partial x^2}\right)_1\right]+\mathcal{O}(\Delta x^2)$$

Zeroth order consistency requires that

$$\alpha = -11-4\gamma_2+\gamma_3$$

and the Taylor series becomes

$$\left(\frac{\partial\lambda}{\partial t}\right)_1 = -U_1\left[\frac{13+8\gamma_2-3\gamma_3}{6}\left(\frac{\partial\lambda}{\partial x}\right)_1-\frac{3+\gamma_3}{4}\Delta x\left(\frac{\partial^2\lambda}{\partial x^2}\right)_1\right]+\mathcal{O}(\Delta x^2)$$

With $\gamma_2, \gamma_3 \in \{0, 1\}$ it is clear that $13+8\gamma_2-3\gamma_3 \neq 6$, and therefore the outflow boundary condition does not achieve first order consistency. This is true even if there is no change in the wind direction near the boundary, i.e. $\gamma_1 = \gamma_2 = \gamma_3 = 0$. However, the effects of this inconsistency will not be felt if there is no source in the adjoint equation near the boundary (the cost functional does not use values near the boundary). In this case for $U_1 < 0$ the boundary condition $\lambda_L = 0$ propagates inside the domain for a finite distance for $t < t^F$. Then $\lambda = 0$ on a whole neighbourhood of the boundary containing grid point 1, and $(\partial^k\lambda/\partial x^k)_1 = 0$. Consequently $\lambda_1(t) =$ and $\partial\lambda_1/\partial t = 0$, which is the correct solution.

A.2. Consistency of finite volume schemes

A.2.1. First order finite volume scheme. We consider the following space discretization of (7) on staggered grids:

$$\frac{\partial C_i}{\partial t} = \frac{F_{i-1/2}-F_{i+1/2}}{\Delta x} \tag{A2}$$

where the first order upwind flux is defined by

$$F_{i-1/2} = \begin{cases} U_{i-1/2}\,C_{i-1} & \text{if } U_{i-1/2} \geqslant 0 \\ U_{i-1/2}\,C_i & \text{if } U_{i-1/2} < 0 \end{cases} \tag{A3}$$

Using the notation

$$\gamma_{i-1/2} = \begin{cases} 1 & \text{if } U_{i-1/2} \geqslant 0 \\ 0 & \text{if } U_{i-1/2} < 0 \end{cases}$$

DOI: 10.1002/fld

scheme (A2) can be written compactly as:

$$\frac{\partial C_i}{\partial t} = \frac{1}{\Delta x}[\gamma_{i-1/2}U_{i-1/2}C_{i-1} + ((1-\gamma_{i-1/2})U_{i-1/2} - \gamma_{i+1/2}U_{i+1/2})C_i - (1-\gamma_{i+1/2})U_{i+1/2}C_{i+1}] \tag{A4}$$

The Dirichlet boundary conditions are use to construct the (inflow) boundary fluxes. For the left boundary we have that

$$F_{1/2} = \begin{cases} U_{1/2}C_{\mathrm{L}} & \text{if } U_{1/2} \geqslant 0 \\ U_{1/2}C_1 & \text{if } U_{1/2} < 0 \end{cases}$$

$$\frac{\partial C_1}{\partial t} = \frac{\Delta t}{\Delta x}[\gamma_{1/2}U_{1/2}C_{\mathrm{L}} + ((1-\gamma_{1/2})U_{1/2} - \gamma_{3/2}U_{3/2})C_1 - (1-\gamma_{3/2})U_{3/2}C_2]$$

and a similar boundary equation is used for the right boundary.

Discrete adjoint scheme: The discrete adjoint of (A4) reads:

$$\begin{aligned} \frac{\partial \lambda_i}{\partial t} &= -\frac{1}{\Delta x}[-(1-\gamma_{i-1/2})U_{i-1/2}\lambda_{i-1} + ((1-\gamma_{i-1/2})U_{i-1/2} - \gamma_{i+1/2}U_{i+1/2})\lambda_i \\ &\quad + \gamma_{i+1/2}U_{i+1/2}\lambda_{i+1}] \\ &= -(1-\gamma_{i-1/2})U_{i-1/2}\frac{\lambda_i - \lambda_{i-1}}{\Delta x} - \gamma_{i+1/2}U_{i+1/2}\frac{\lambda_{i+1} - \lambda_i}{\Delta x} \end{aligned} \tag{A5}$$

The discrete adjoint (A5) is an upwind discretization of the continuous adjoint equation. A formal Taylor series expansion around the centre point of grid i leads to:

$$\left(\frac{\partial \lambda}{\partial t}\right)_i = -(1 + \gamma_{i+1/2} - \gamma_{i-1/2})U_i\left(\frac{\partial \lambda}{\partial x}\right)_i + \mathcal{O}(\Delta x)$$

If the wind does not change direction within cell i then $\gamma_{i+1/2} - \gamma_{i-1/2} = 0$ and (A5) is a first order consistent discretization of the continuous adjoint. If the wind changes direction then (A5) is not consistent with the continuous adjoint. For a sink ($U_{i-1/2} \geqslant 0$ and $U_{i+1/2} < 0$) the time derivative of λ_i is zero. For a source ($U_{i-1/2} < 0$ and $U_{i+1/2} \geqslant 0$) the time derivative of λ_i is driven by contributions from both boundaries.

The boundary condition for the adjoint equation is:

$$\lambda_{\mathrm{L}} = 0 \quad \text{if } U_{1/2} < 0$$
$$\lambda_{\mathrm{R}} = 0 \quad \text{if } U_{N+1/2} \geqslant 0$$

DOI: 10.1002/fld

The discrete adjoint scheme at the left boundary reads

$$\frac{\partial \lambda_1}{\partial t} = \frac{1}{\Delta x}[((1-\gamma_{1/2})U_{1/2} - \gamma_{3/2}U_{3/2})\lambda_1 + \gamma_{3/2}U_{3/2}\lambda_2]$$
$$= \frac{1}{\Delta x}[-(1-\gamma_{1/2})U_{1/2}\lambda_{\mathrm{L}} + ((1-\gamma_{1/2})U_{1/2} - \gamma_{3/2}U_{3/2})\lambda_1 + \gamma_{3/2}U_{3/2}\lambda_2] \quad \text{(A6)}$$

and a similar relation holds for the left boundary. From the previous analysis we infer that if there is no change of wind direction at the edges of the boundary cell ($\gamma_{1/2} = \gamma_{3/2}$) then the discrete adjoint boundary condition is consistent at both inflow and outflow boundaries.

A.2.2. Second order finite volume scheme. Forward scheme: We now consider the space semi-discretization (A2) on staggered grids with the following flux interpolation:

$$F_{i-1/2} = \begin{cases} \dfrac{U_{i-1/2}}{6}(-C_{i-2} + 5C_{i-1} + 2C_i) & \text{if } U_{i-1/2} \geqslant 0 \\ \dfrac{U_{i-1/2}}{6}(2C_{i-1} + 5C_i - C_{i+1}) & \text{if } U_{i-1/2} < 0 \end{cases}$$
$$= \frac{U_{i-1/2}}{6}(-\gamma_{i-1/2}C_{i-2} + (2+3\gamma_{i-1/2})C_{i-1} + (5-3\gamma_{i-1/2})C_i$$
$$-(1-\gamma_{i-1/2})C_{i+1}) \quad \text{(A7)}$$

This leads to the following scheme (in compact notation):

$$\frac{\partial C_i}{\partial t} = \frac{1}{6\Delta x}[-\gamma_{i-1/2}U_{i-1/2}C_{i-2} + ((2+3\gamma_{i-1/2})U_{i-1/2} + \gamma_{i+1/2}U_{i+1/2})C_{i-1}$$
$$+ ((5-3\gamma_{i-1/2})U_{i-1/2} - (2+3\gamma_{i+1/2})U_{i+1/2})C_i$$
$$+ (-(1-\gamma_{i-1/2})U_{i-1/2} - (5-3\gamma_{i+1/2})U_{i+1/2})C_{i+1}$$
$$+ (1-\gamma_{i+1/2})U_{i+1/2}C_{i+2}] \quad \text{(A8)}$$

This numerical scheme is upwind biased, third order accurate for constant wind velocity, and second order accurate for general flux functions (including non-constant velocity).

Since the stencil is large a different numerical scheme is used near the boundary. We now consider the numerical treatment of the left boundary; similar formulas can be given for the right boundary

$$F_{1/2} = \begin{cases} U_{1/2}C_{\mathrm{L}} & \text{if } U_{1/2} \geqslant 0 \\ U_{1/2}\left[\dfrac{3}{2}C_1 - \dfrac{1}{2}C_2\right] & \text{if } U_{1/2} < 0 \end{cases}$$
$$= \frac{U_{1/2}}{6}(6\gamma_{1/2}C_{\mathrm{L}} + 9(1-\gamma_{1/2})C_1 - 3(1-\gamma_{1/2})C_2) \quad \text{(A9)}$$

DOI: 10.1002/fld

$$F_{3/2} = \begin{cases} U_{3/2}\left(\frac{1}{2}C_1 + \frac{1}{2}C_2\right) & \text{if } U_{3/2} \geqslant 0 \\ U_{3/2}\left(\frac{1}{3}C_1 + \frac{5}{6}C_2 - \frac{1}{6}C_3\right) & \text{if } U_{3/2} < 0 \end{cases}$$

$$= \frac{U_{3/2}}{6}((2+\gamma_{3/2})C_1 + (5-2\gamma_{3/2})C_2 - (1-\gamma_{3/2})C_3) \tag{A10}$$

At the nodes near the boundary the solution evolves according to:

$$\frac{\partial C_1}{\partial t} = \frac{1}{6\Delta x}[6\gamma_{1/2}U_{1/2}C_{\mathrm{L}} + (9(1-\gamma_{1/2})U_{1/2} - (2+\gamma_{3/2})U_{3/2})C_1 + (-3(1-\gamma_{1/2})U_{1/2} - (5-2\gamma_{3/2})U_{3/2})C_2 + (1-\gamma_{3/2})U_{3/2}C_3]$$

$$\frac{\partial C_2}{\partial t} = \frac{1}{6\Delta x}[((2+\gamma_{3/2})U_{3/2} + \gamma_{5/2}U_{5/2})C_1 + ((5-2\gamma_{3/2})U_{3/2} - (2+3\gamma_{5/2})U_{5/2})C_2 + (-(1-\gamma_{3/2})U_{3/2} - (5-3\gamma_{5/2})U_{5/2})C_3 + (1-\gamma_{5/2})U_{5/2}C_4]$$

Discrete adjoint scheme: The discrete adjoint of the finite volume scheme for the nodes inside the domain is:

$$\frac{\partial \lambda_i}{\partial t} = -\frac{1}{6\Delta x}[(1-\gamma_{i-3/2})U_{i-3/2}\lambda_{i-2} - ((1-\gamma_{i-3/2})U_{i-3/2} + (5-3\gamma_{i-1/2})U_{i-1/2})\lambda_{i-1} + ((5-3\gamma_{i-1/2})U_{i-1/2} - (2+3\gamma_{i+1/2})U_{i+1/2})\lambda_i + ((2+3\gamma_{i+1/2})U_{i+1/2} + \gamma_{i+3/2}U_{i+3/2})\lambda_{i+1} - \gamma_{i+3/2}U_{i+3/2}\lambda_{i+2}]$$

This is an upwind discretization of the continuous adjoint equation. A Taylor series around x_i reveals that:

$$\left(\frac{\partial \lambda}{\partial t}\right)_i = -U_i\left(\frac{\partial \lambda}{\partial x}\right)_i + \frac{3\gamma_{i-1/2} - \gamma_{i-3/2} - 3\gamma_{i+1/2} + \gamma_{i+3/2}}{6}U_i\left(\frac{\partial \lambda}{\partial x}\right)_i - \frac{\gamma_{i-1/2} - \gamma_{i-3/2} + \gamma_{i+1/2} - \gamma_{i+3/2}}{4}\left(\left(\frac{\partial \lambda}{\partial x}\right)_i\left(\frac{\partial U}{\partial x}\right)_i + \left(\frac{\partial^2 \lambda}{\partial x^2}\right)_i U_i\right)\Delta x + \frac{2+3\gamma_{i-1/2} - 9\gamma_{i-3/2} - 3\gamma_{i+1/2} + 9\gamma_{i+3/2}}{24}\left(\frac{\partial U}{\partial x}\right)_i\left(\frac{\partial^2 \lambda}{\partial x^2}\right)_i \Delta x^2 + \frac{2+3\gamma_{i-1/2} - 9\gamma_{i-3/2} - 3\gamma_{i+1/2} + 9\gamma_{i+3/2}}{48}\left(\frac{\partial \lambda}{\partial x}\right)_i\left(\frac{\partial^2 U}{\partial x^2}\right)_i \Delta x^2$$

DOI: 10.1002/fld

$$+\frac{3\gamma_{i-1/2}-7\gamma_{i-3/2}-3\gamma_{i+1/2}+7\gamma_{i+3/2}}{36}\left(\frac{\partial\lambda^3}{\partial x^3}\right)_i U_i\,\Delta x^2+\mathcal{O}(\Delta x^3)$$

The consistency conditions are:

$$\text{order 1:}\quad 3\gamma_{i-1/2}-\gamma_{i-3/2}-3\gamma_{i+1/2}+\gamma_{i+3/2}=0$$

$$\text{order 2:}\quad \gamma_{i-1/2}-\gamma_{i-3/2}+\gamma_{i+1/2}-\gamma_{i+3/2}=0$$

If the wind does not change direction within the cells $i-1, i, i+1$ (i.e. $\gamma_{i-3/2}=\gamma_{i-1/2}=\gamma_{i+1/2}=\gamma_{i+3/2}$) then the adjoint scheme is second order consistent in general, and third order consistent for constant wind velocity. The discrete adjoint scheme is only first order consistent if $\gamma_{i-3/2}=\gamma_{i+3/2}\neq\gamma_{i-1/2}=\gamma_{i+1/2}$ (e.g. $U_{i-3/2}, U_{i+3/2}<0$ and $U_{i-1/2}, U_{i+1/2}\geqslant 0$ or *vice versa*). For all other wind direction patterns (e.g. $U_{i-3/2}<0$ and $U_{i-1/2}, U_{i+1/2}, U_{i+3/2}\geqslant 0$) the scheme is inconsistent.

The discrete adjoint left boundary relations are:

$$\begin{aligned}\frac{\partial\lambda_1}{\partial t}&=-\frac{1}{6\Delta x}[(9(1-\gamma_{1/2})U_{1/2}-(2+\gamma_{3/2})U_{3/2})\lambda_1\\&\quad+((2+\gamma_{3/2})U_{3/2}+\gamma_{5/2}U_{5/2})\lambda_2-\gamma_{5/2}U_{5/2}\lambda_3]\\&=-\frac{9(1-\gamma_{1/2})}{6}U_{1/2}\frac{\lambda_1-\lambda_0}{\Delta x}-\frac{2+\gamma_{3/2}}{6}U_{3/2}\frac{\lambda_2-\lambda_1}{\Delta x}-\frac{\gamma_{5/2}}{6}U_{5/2}\frac{\lambda_3-\lambda_2}{\Delta x}\end{aligned}$$

The left boundary condition $\lambda_0=0$ only enters the solution when $\gamma_{1/2}=0$. The Taylor series around x_1

$$\left(\frac{\partial\lambda}{\partial t}\right)_1=-\left(\frac{11-9\gamma_{1/2}+\gamma_{3/2}-\gamma_{5/2}}{6}\right)U_1\left(\frac{\partial\lambda}{\partial x}\right)_1+\mathcal{O}(\Delta x)$$

reveals that the scheme for λ_1 is inconsistent with the continuous adjoint equation for any upwinding situation, since $9\gamma_{1/2}-\gamma_{3/2}+\gamma_{52}\neq 5$ for any combination of $\gamma_j\in\{0,1\}$.

Similarly, for the second node from the boundary

$$\begin{aligned}\frac{\partial\lambda_2}{\partial t}&=-\frac{1}{6\Delta x}[(-3(1-\gamma_{1/2})U_{1/2}-(5-2\gamma_{3/2})U_{3/2})\lambda_1+((5-2\gamma_{3/2})U_{3/2}-(2+3\gamma_{5/2})U_{52})\lambda_2\\&\quad+((2+3\gamma_{5/2})U_{5/2}+\gamma_{7/2}U_{7/2})\lambda_3-\gamma_{7/2}U_{7/2}\lambda_4]\\&=-\frac{4+3\gamma_{1/2}-2\gamma_{3/2}+3\gamma_{5/2}-\gamma_{7/2}}{6}U_2\left(\frac{\partial\lambda}{\partial x}\right)_2+\mathcal{O}(\Delta x)\end{aligned}$$

The relation is consistent only for particular patterns of wind directions ($\gamma_{1/2}=\gamma_{5/2}=1$, $\gamma_{3/2}=\gamma_{7/2}=0$ or $\gamma_{1/2}=\gamma_{7/2}=1$, $\gamma_{3/2}=\gamma_{5/2}=0$ or $\gamma_{1/2}=\gamma_{3/2}=0$, $\gamma_{5/2}=\gamma_{7/2}=1$). The scheme is not consistent, however, if the wind does not change direction near the boundary.

DOI: 10.1002/fld

A.3. Consistency of MUSCL with slope limiting

In this section we analyse the consistency of the MUSCL slope-limited scheme. To simplify the analysis we assume that there is a single jump discontinuity in the forward solution, and that the slope limiter is active only in the ith cell. The general case where the slope limiter takes different values in different cells can be treated similarly.

It is clear from (28) and (29) that in the forward scheme the solution is first slope-limited and then advanced in time, but in the discrete adjoint scheme these steps are reversed. Our analysis on the adjoint scheme for finite differences and finite volumes method revealed that the (backward in) time advancement operator A^{T} does not introduce any inconsistency. Therefore we focus on the adjoint of the limiter operator.

In the adjoint solution λ_C is the costate variable associated with C, and λ_S the costate associated with S. The case without slope limiter corresponds to $L(C, S) = S$. The adjoint solution is first propagated (backward in time) with the operator A^{T}

$$\begin{aligned}(\overline{\lambda}_C)_i^n &= (1-\sigma)(\lambda_C)_i^{n+1} + \sigma(\lambda_C)_{i+1}^{n+1} + 12\delta(\lambda_S)_i^{n+1} - 12\delta(\lambda_S)_{i+1}^{n+1}\\ (\overline{\lambda}_S)_i^n &= -\delta(\lambda_C)_i^{n+1} + \delta(\lambda_C)_{i+1}^{n+1} + \alpha(\lambda_S)_i^{n+1} + \beta(\lambda_S)_{i+1}^{n+1}\end{aligned} \tag{A11}$$

and the corrected by the adjoint of the forward limiter

$$\lambda_C^n = \overline{\lambda}_C^n + \left(\frac{\partial L(C^n, S^n)}{\partial C^n}\right)^{\mathrm{T}} \overline{\lambda}_S^n, \quad \lambda_S^n = \left(\frac{\partial L(C^n, S^n)}{\partial S^n}\right)^{\mathrm{T}} \overline{\lambda}_S^n$$

The discretization of the continuous adjoint equation with (25) leads to the following scheme:

$$\begin{aligned}(\overline{\lambda}_S)_i^{n+1} &= L((\lambda_C)_i^{n+1}, (\lambda_S)_i^{n+1})\\ (\lambda_C)_i^n &= (1-\sigma)(\lambda_C)_i^{n+1} + \sigma(\lambda_C)_{i+1}^{n+1} - \delta(\overline{\lambda}_S)_i^{n+1} + \delta(\overline{\lambda}_S)_{i+1}^{n+1}\\ (\lambda_S)_i^{n+1} &= \alpha(\overline{\lambda}_S)_i^{n+1} + \beta(\overline{\lambda}_S)_{i+1}^{n+1} + 12\delta(\lambda_C)_i^{n+1} - 12\delta(\lambda_C)_{i+1}^{n+1}\end{aligned}$$

We next discuss the adjoint solution for each of the four possible values assumed by the slope limiter.

Case 1: The slope is not changed, therefore, this case covers the unlimited situation as well

$$\overline{S}_i = S_i^n \quad \Rightarrow \quad (\lambda_C)_i^n = (\overline{\lambda}_C)_i^n, \quad (\lambda_S)_i^n = (\overline{\lambda}_S)_i^n \tag{A12}$$

In this case the consistency of the adjoint is automatic.

Case 2:

$$\begin{aligned}\overline{S}_i &= \tfrac{3}{2}(C_i^n - C_{i-1}^n)\\ (\lambda_C)_j^n &= (\overline{\lambda}_C)_j^n \quad \text{for } j \neq i-1, i\\ (\lambda_C)_i^n &= (\overline{\lambda}_C)_i^n + \tfrac{3}{2}(\overline{\lambda}_S)_i^n\\ &= (\overline{\lambda}_C)_i^n + \tfrac{3}{2}\delta[(\lambda_C)_{i+1}^{n+1} - (\lambda_C)_i^{n+1}] + \tfrac{3}{2}\alpha(\lambda_S)_i^{n+1} + \tfrac{3}{2}\beta(\lambda_S)_{i+1}^{n+1}\end{aligned}$$

DOI: 10.1002/fld

$$
\begin{aligned}
&= (1 - [\sigma + \tfrac{3}{2}\delta])(\lambda_C)_i^{n+1} + (\sigma + \tfrac{3}{2}\delta)(\lambda_C)_{i+1}^{n+1} \\
&\quad + (12\delta + \tfrac{3}{2}\alpha)(\lambda_S)_i^{n+1} - (12\delta - \tfrac{3}{2}\beta)(\lambda_S)_{i+1}^{n+1} \qquad \text{(A13)} \\
(\lambda_C)_{i-1}^n &= (\overline{\lambda}_C)_{i-1}^n - \tfrac{3}{2}(\overline{\lambda}_S)_i^n \\
&= (\overline{\lambda}_C)_{i-1}^n - \tfrac{3}{2}\delta[(\lambda_C)_{i+1}^{n+1} - (\lambda_C)_i^{n+1}] - \tfrac{3}{2}\alpha(\lambda_S)_i^{n+1} - \tfrac{3}{2}\beta(\lambda_S)_{i+1}^{n+1} \\
&= (1 - [\sigma - \tfrac{3}{2}\delta])(\lambda_C)_{i-1}^{n+1} + (\sigma - \tfrac{3}{2}\delta)(\lambda_C)_i^{n+1} \\
&\quad - \tfrac{3}{2}\delta[(\lambda_C)_{i-1}^{n+1} - 2(\lambda_C)_i^{n+1} + (\lambda_C)_{i+1}^{n+1}] \\
&\quad + 12\delta(\lambda_S)_{i-1}^{n+1} - (12\delta + \tfrac{3}{2}\alpha)(\lambda_S)_i^{n+1} - \tfrac{3}{2}\beta(\lambda_S)_{i+1}^{n+1} \\
(\lambda_S)_i^n &= 0, \quad (\lambda_S)_j^n = (\overline{\lambda}_S)_j^n \text{ for } j \neq i
\end{aligned}
$$

A comparison of (A13) with the scheme without limiter (A11) reveals the effect of slope limiting on the adjoint: the local Courant number is changed from σ to $\sigma + 3\delta/2$ in cell i, and from σ to $\sigma - 3\delta/2$ in cell $i-1$. In addition a diffusion-like term is added to $i-1$; for smooth adjoints this term is $O(\Delta x^2)$. As a result of the slope limiter the local adjoint propagation speed is increased in cell i, and is decreased by the same amount in cell $i-1$. The mass inflow into cell $i-1$ exceeds the mass outflow, but the mass inflow into cell i is smaller than the mass outflow. As a result we expect a wiggle to form in the adjoint solution between cells $i-1$ and i.

Since $\delta = \sigma(1-\sigma)/2$, and the original Courant number $\sigma \in [0, 1]$, the modified Courant numbers are also positive and smaller, than one, $\sigma \pm 3\delta/2 \in [0, 1]$. The modified speeds have the same sign as the original speed, and the new Courant numbers do not exceed one, consequently no additional stability conditions are necessary.

Case 3:

$$
\begin{aligned}
\overline{S}_i &= \tfrac{3}{2}(C_{i+1}^n - C_i^n) \\
(\lambda_C)_i^n &= (\overline{\lambda}_C)_i^n - \tfrac{3}{2}(\overline{\lambda}_S)_i^n \\
&= (\overline{\lambda}_C)_i^n - \tfrac{3}{2}\delta[(\lambda_C)_{i+1}^{n+1} - (\lambda_C)_i^{n+1}] - \tfrac{3}{2}\alpha(\lambda_S)_i^{n+1} - \tfrac{3}{2}\beta(\lambda_S)_{i+1}^{n+1} \\
&= (1 - [\sigma - \tfrac{3}{2}\delta])(\lambda_C)_i^{n+1} + (\sigma - \tfrac{3}{2}\delta)(\lambda_C)_{i+1}^{n+1} \\
&\quad + (12\delta - \tfrac{3}{2}\alpha)(\lambda_S)_i^{n+1} - (12\delta + \tfrac{3}{2}\beta)(\lambda_S)_{i+1}^{n+1} \\
(\lambda_C)_{i+1}^n &= (\overline{\lambda}_C)_{i+1}^n + \tfrac{3}{2}(\overline{\lambda}_S)_i^n \\
&= (\overline{\lambda}_C)_{i+1}^n + \tfrac{3}{2}\delta[(\lambda_C)_{i+1}^{n+1} - (\lambda_C)_i^{n+1}] + \tfrac{3}{2}\alpha(\lambda_S)_i^{n+1} + \tfrac{3}{2}\beta(\lambda_S)_{i+1}^{n+1} \qquad \text{(A14)} \\
&= -\tfrac{3}{2}\delta(\lambda_C)_i^{n+1} + (1 - [\sigma - \tfrac{3}{2}\delta])(\lambda_C)_{i+1}^{n+1} + \sigma(\lambda_C)_{i+2}^{n+1} \\
&\quad + \tfrac{3}{2}\alpha(\lambda_S)_i^{n+1} + (12\delta + \tfrac{3}{2}\beta)(\lambda_S)_{i+1}^{n+1} - 12\delta(\lambda_S)_{i+2}^{n+1}
\end{aligned}
$$

DOI: 10.1002/fld

$$
\begin{aligned}
&= (1 - [\sigma + \tfrac{3}{2}\delta])(\lambda_C)_{i+1}^{n+1} + (\sigma + \tfrac{3}{2}\delta)(\lambda_C)_{i+2}^{n+1} \\
&\quad - \tfrac{3}{2}\delta[(\lambda_C)_i^{n+1} - 2(\lambda_C)_{i+1}^{n+1} + (\lambda_C)_{i+2}^{n+1}] \\
&\quad + \tfrac{3}{2}\alpha(\lambda_S)_i^{n+1} + (12\delta + \tfrac{3}{2}\beta)(\lambda_S)_{i+1}^{n+1} - 12\delta(\lambda_S)_{i+2}^{n+1} \\
(\lambda_S)_i^n &= 0
\end{aligned}
$$

A comparison of (A14) with the scheme without limiter (31) reveals the effect of slope limiting on the adjoint: the local Courant number is changed from σ to $\sigma - 3\delta/2$ in cell i, and from σ to $\sigma + 3\delta/2$ in cell $i+1$. Since $\delta = \sigma(1-\sigma)/2$, and the original Courant number $\sigma \in [0, 1]$, the modified Courant numbers are also positive and smaller than one since $\sigma \pm 3\delta/2 \in [0, 1]$.

Case 4:

$$
\overline{S}_i = 0 \;\Rightarrow\; (\lambda_C)_i^n = (\overline{\lambda}_C)_i^n, \quad (\lambda_S)_i^n = 0 \tag{A15}
$$

In this case the adjoint of the concentration is not changed, the discrete adjoint is a consistent low order discretization.

A.4. Discrete adjoints of flux-limited scheme

In this section we derive the discrete adjoint of the flux-limited forward scheme. In matrix form the forward scheme (32) is

$$
\begin{aligned}
F^n &= uC^n + \frac{u(1-\sigma)}{2}\,\Phi \cdot (-\mathscr{D}^{\mathrm{T}}) \cdot C^n \\
C^{n+1} &= C^n - \frac{\Delta t}{\Delta x}\mathscr{D} \cdot F^n \\
&= C^n - \sigma\,\mathscr{D} \cdot C^n + \frac{\sigma(1-\sigma)}{2}(\mathscr{D} \cdot \Phi \cdot \mathscr{D}^{\mathrm{T}}) \cdot C^n
\end{aligned} \tag{A16}
$$

where F is the vector of cell boundary fluxes, $\mathscr{D}$ is the backward finite difference operator, $-\mathscr{D}^{\mathrm{T}}$ is the forward finite difference operator, and Φ is a diagonal matrix with the limiter values on the diagonal,

$$
F = \begin{bmatrix} F_{3/2} \\ \vdots \\ F_{N+\frac{1}{2}} \end{bmatrix}, \quad
\mathscr{D} = \begin{bmatrix} 1 & 0 & \cdots & -1 \\ -1 & 1 & \cdots & 0 \\ 0 & \ddots & \ddots & 0 \\ 0 & 0 & -1 & 1 \end{bmatrix}, \quad
\Phi = \begin{bmatrix} \phi(r_{3/2}) & \cdots & 0 \\ 0 & \ddots & 0 \\ 0 & \cdots & \phi(r_{N+1/2}) \end{bmatrix}
$$

The tangent linear model of (A16) is

$$
\delta C^{n+1} = \left[I - \sigma\mathscr{D} + \frac{\sigma(1-\sigma)}{2}\,\mathscr{D} \cdot (\Phi \cdot \mathscr{D}^{\mathrm{T}} \cdot C^n)' \right] \delta C^n
$$

DOI: 10.1002/fld

where $(\Phi \cdot \mathscr{D}^{\mathrm{T}} \cdot C^n)'$ is the Jacobian of $\Phi \cdot \mathscr{D}^{\mathrm{T}} \cdot C^n$ with respect to C^n. The corresponding discrete adjoint scheme reads

$$\begin{aligned}\lambda^n &= \left[I - \sigma\mathscr{D} + \frac{\sigma(1-\sigma)}{2}\, \mathscr{D} \cdot (\Phi \cdot \mathscr{D}^{\mathrm{T}} \cdot C^n)' \right]^{\mathrm{T}} \lambda^{n+1} \\ &= \lambda^{n+1} - \sigma\mathscr{D}^{\mathrm{T}}\lambda^{n+1} \\ &\quad + \frac{\sigma(1-\sigma)}{2}[(\Phi \cdot (-\mathscr{D}^{\mathrm{T}}) \cdot C^n)']^{\mathrm{T}} \cdot (-\mathscr{D}^{\mathrm{T}}) \cdot \lambda^{n+1}\end{aligned} \tag{A17}$$

In component-wise notation we have

$$\begin{aligned}\frac{\partial(\Phi \cdot (-\mathscr{D}^{\mathrm{T}}) \cdot C)_i}{\partial C_j} &= \frac{\partial(\phi(r_{i+1/2})(C_{i+1} - C_i))}{\partial C_j} \\ &= \phi(r_{i+1/2}) \frac{\partial\,(C_{i+1} - C_i)}{\partial C_j} \\ &\quad + \phi_r(r_{i+1/2})\, \frac{\partial r_{i+1/2}}{\partial C_j}\, (C_{i+1} - C_i)\end{aligned} \tag{A18}$$

In the above we denote $\phi_r = \partial\phi/\partial r$. From (37) we have

$$\frac{\partial r_{i+1/2}}{\partial C_j} = \begin{cases} -1/(C_{i+1} - C_i) & \text{for } j = i-1 \\ (1 + r_{i+1/2})/(C_{i+1} - C_i) & \text{for } j = i \\ -r_{i+1/2}/(C_{i+1} - C_i) & \text{for } j = i+1 \\ 0 & \text{otherwise} \end{cases}$$

In matrix notation the Jacobian is

$$(\Phi \cdot (-\mathscr{D}^{\mathrm{T}}) \cdot C^n)' = \Phi \cdot (-\mathscr{D}^{\mathrm{T}}) + (\Phi_r) \cdot G$$

where (Φ_r) is a diagonal matrix with $(\Phi_r)_{ii} = \phi_r(r_{i+1/2})$ and

$$G = \begin{bmatrix} 1 + r_{3/2} & -r_{3/2} & 0 & \cdots & -1 \\ -1 & 1 + r_{5/2} & -r_{5/2} & & \\ & \ddots & \ddots & \ddots & \\ & -1 & 1 + r_{i+1/2} & -r_{i+1/2} & \\ & & \ddots & \ddots & \ddots \\ -r_{N+1/2} & 0 & \cdots & -1 & 1 + r_{N+1/2} \end{bmatrix}$$

DOI: 10.1002/fld

The adjoint scheme (A17) reads

$$\lambda^n = \lambda^{n+1} - \sigma \mathscr{D}^{\mathrm{T}} \lambda^{n+1} - \frac{\sigma(1-\sigma)}{2} \mathscr{D} \cdot \Phi \cdot (-\mathscr{D}^{\mathrm{T}}) \cdot \lambda^{n+1} + \frac{\sigma(1-\sigma)}{2} G^{\mathrm{T}} \cdot (\Phi_r) \cdot (-\mathscr{D}^{\mathrm{T}}) \cdot \lambda^{n+1} \tag{A19}$$

In the pointwise formulation the discrete adjoint (A19) is

$$\begin{aligned} \lambda_i^n = {} & \lambda_i^{n+1} + \sigma(\lambda_{i+1}^{n+1} - \lambda_i^{n+1}) \\ & - \frac{\sigma(1-\sigma)}{2}[(\phi - r\phi_r)_{i+1/2}^n (\lambda_{i+1}^{n+1} - \lambda_i^{n+1}) - (\phi - r\phi_r)_{i-1/2}^n (\lambda_i^{n+1} - \lambda_{i-1}^{n+1})] \\ & - \frac{\sigma(1-\sigma)}{2}[(\phi_r)_{i+3/2}^n (\lambda_{i+2}^{n+1} - \lambda_{i+1}^{n+1}) - (\phi_r)_{i+1/2}^n (\lambda_{i+1}^{n+1} - \lambda_i^{n+1})] \end{aligned}$$

ACKNOWLEDGEMENTS

This work was supported by the National Science Foundation through the awards CAREER ACI-0413872 and ITR AP&IM-0205198. The authors thank the two anonymous reviewers for their constructive comments.

REFERENCES

1. Sandu A, Daescu DN, Carmichael GR, Chai T. Adjoint sensitivity analysis of regional air quality models. *Journal of Computational Physics* 2005; **204**:222–252.
2. Daley R. *Atmospheric Data Analysis*. Cambridge University Press: Cambridge, 1991.
3. Cacuci DG. Sensitivity theory for nonlinear systems. I. Nonlinear functional analysis approach. *Journal of Mathematical Physics* 1981; **22**:2794–2802.
4. Sirkes Z, Tziperman E. Finite difference of adjoint or adjoint of finite difference?. *Monthly Weather Review* 1997; **49**:5–40.
5. Griewank A. Evaluating derivatives: principles techniques of algorithmic differentiation. *Frontiers in Applied Mathematics*, vol. 41. SIAM: Philadelphia, 2000.
6. Osher S, Solomon F. Upwind difference-schemes for hyperbolic systems of conservation-laws. *Mathematics of Computation* 1982; **38**(158):339–374.
7. Rood RB. Numerical advection algorithms and their role in atmospheric transport and chemistry models. *Reviews of Geophysics* 1987; **25**(1):71–100.
8. LeVeque RJ. *Finite Volume Methods for Hyperbolic Problems*. Cambridge University Press: Cambridge, 2002.
9. Ulbrich S. Adjoint-based derivative computations for the optimal control of discontinuous solutions of hyperbolic conservation laws. *Systems and Control Letters* 2003; **48**:313–328.
10. Xu Q. Generalized adjoint for physical processes with parameterized discontinuities. Part I: Basic issues and heuristic examples. *Journal of the Atmospheric Sciences* 1996; **53**(8):1123–1142.
11. Akella S, Navon IM. A comparative study of the performance of high resolution advection schemes in the context of data assimilation. *International Journal for Numerical Methods in Fluids* 2006; **51**:719–748.
12. Giles MB. Discrete adjoint approximations with shocks. *Technical Report 02/10*, Oxford University Computing Laboratory, Numerical Analysis Group, 2002.
13. Giles MB, Duta MC, Pierce NA. Algorithm developments for discrete adjoint methods. *AIAA Journal* 2003; **41**(2):198–205.

DOI: 10.1002/fld

14. Ulbrich S. Optimal control of nonlinear hyperbolic conservation laws with source terms. *Habilitation Thesis*, Department of Mathematics, Technical University Munich, 2001.
15. Sei A, Symes W. A note on consistency and adjointness of numerical schemes. *Technical Report CSRPC-TR95527*, Center for Research in Parallel Computation, Rice University, January 1995.
16. Thuburn J, Haine TWN. Adjoint of nonoscillatory advection schemes. *Journal of Computational Physics* 2001; **171**:616–631.
17. Duivesteijn GF, Bijl H, Koren B, van Brummelen EH. On the adjoint solution of the quasi-1D Euler equations: the effect of boundary conditions and the numerical flux function. *International Journal for Numerical Methods in Fluids* 2005; **47**:987–993.
18. Hartmann R. Derivation of an adjoint consistent discontinuous Galerkin discretisation of the compressible Euler equations. *Proceedings BAIL 2006 Conference*, Gottingen, Germany. http://www.num.math.uni-goettingen.de/bail/documents/proceedings/hartmann.pdf.
19. Collis S, Heinkenschloss M. Upwind/Petrov Galerkin method applied to the solution of optimal control problems. *Technical Report TR02-01*, Department of Computational and Applied Mathematics, Rice University, Houston, TX, 2002.
20. Bartlett RA, Heinkenschloss M, Ridzal D, van BloemenWaanders BG. Domain decomposition methods for advection dominated linear quadratic elliptic optimal control problem. *Computer Methods in Applied Mechanics and Engineering* 2006; **195**(44–47):6428–6447.
21. Adcroft A, Campin J-M. Heimbach P, Hill C, Marshall J. *MITGCM Manual*. http://mitgcm.org/sealion/online_documents/manual.pdf, 2002; 449.
22. Burns JA, Ito K, Propst G. On nonconvergence of adjoint semigroups for control systems with delays. *SIAM Journal on Control and Optimization* 1988; **26**(6):1442–1454.
23. Borggaard J, Burns JA, Vugrin E, Zietsman L. On strong convergence of feedback operators for non-normal distributed parameter systems. *Technical Report*, Center for Optimal Design and Control, Interdisciplinary Center for Applied Math, Virginia Tech, Blacksburg, VA, 2004.
24. Homescu C, Navon IM. Optimal control of flow with discontinuities. *Journal of Computational Physics* 2003; **187**:660–682.
25. Vukicevic T, Steyskal M, Hecht M. Properties of advection algorithms in the context of variational data assimilation. *Monthly Weather Review* 2001; **129**(5):1221–1231.
26. Hundsdorfer WH, Verwer JG. *Numerical Solution of Time-Dependent Advection–Diffusion–Reaction Equations*. Springer Series in Computational Mathematics, vol. 33. Springer: Berlin, 2003.
27. Colella P, Woddward PR. The piecewise parabolic method (PPM) for gas-dynamical simulations. *Journal of Computational Physics* 1984; **54**:174–201.
28. van Leer B. Towards the ultimate conservative difference scheme IV. A new approach to numerical convection. *Journal of Computational Physics* 1977; **23**:276–299.
29. Sweby PK. High resolution schemes using flux limiters for hyperbolic conservation laws. *SIAM Journal on Numerical Analysis* 1984; **21**:995–1011.
30. Byrd R, Lu P, Nocedal J. A limited memory algorithm for bound constrained optimization. *SIAM Journal on Scientific and Statistical Computing* 1995; **16**(5):1190–1208.
31. Gosse L, James F. Numerical approximations of one-dimensional linear conservation equations with discontinuous coefficients. *Mathematics of Computation* 2000; **69**(231):987–1015.
32. Laney CB. *Computational Gas Dynamics*. Cambridge University Press: Cambridge, 1998.
33. Toro EF. *Riemman Solvers and Numerical Methods for Fluid Dynamics* (2nd edn). Springer: Berlin, 1999.

DOI: 10.1002/fld